Confocal microscopy

HEK293 cells (2.0×10^5 cells/well) were plated onto poly-L-lysine–coated micro coverglasses (BD Biosciences) in a 24-well plate. The following day, cells were transfected with the indicated plasmids using FuGENE HD. Twenty-four hours after transfection, cells were washed twice with PBS, fixed with 4% paraformaldehyde for 15 min, and permeabilized with PBS containing 100 μg/ml digitonin and 1% BSA. In the case of human macrophages, fixed cells (2.5×10^4 cells/well) were permeabilized with PBS containing 0.1% Triton X-100 and 2% BSA for 15 min. Fixed cells were blocked in PBS containing 1% BSA and labeled with the indicated primary Abs (2–10 μg/ml) for 60 min at room temperature. Alexa Fluor–conjugated secondary Abs (1:400) were used to visualize the staining of the primary Abs. After mounting with ProLong Gold with DAPI (Molecular Probes), cells were visualized at ×63 magnification with an LSM510 META microscope (Zeiss, Jena, Germany).

Results

Insertion loop between LRR14 and LRR15 is indispensable for hTLR8-mediated signaling

To examine the requirement of proteolytic processing in ligand recognition and signaling by hTLR8, C-terminal FLAG-tagged wild-type TLR8 and truncated mutant forms were provided. TLR8Δloop lacks the insertion loop between LRR14 and LRR15. TLR8-C represents a deletion mutant lacking LRR1–14 and the insertion loop. These were transiently expressed in HEK293 cells and stimulated with a synthetic small molecule (CL075) and ssRNA40 complexed to DOTAP. Wild-type TLR8 was expressed at the expected molecular mass (~150 kDa) and activated NF-κB in response to CL075, but not to ssRNA40, whereas TLR8Δloop failed to respond to both ligands (Fig. 1A, 1B). Cleavage products of TLR8 were undetectable in HEK293 cell lysates in either type of TLR8 expression (Fig. 1B). In addition, TLR8-C did not activate NF-κB in response to CL075 and ssRNA40 (Fig. 1A, 1B).

UNC93B1 physically associates with hTLR8 and regulates intracellular trafficking and signaling of TLR8 (10). When UNC93B1 was coexpressed with wild-type TLR8 in HEK293 cells, CL075-induced TLR8-mediated NF-κB activation was greatly increased concomitantly with the appearance of the N- and C-terminal halves of TLR8, but no response to ssRNA40 was observed (Fig. 1C, 1D). The molecular mass of the C-terminal half of TLR8 was almost the same as that of TLR8-C. In contrast, TLR8Δloop that remained uncleaved could not respond to CL075 or ssRNA40 even though it was coexpressed with UNC93B1 (Fig. 1C, 1D). Again, the

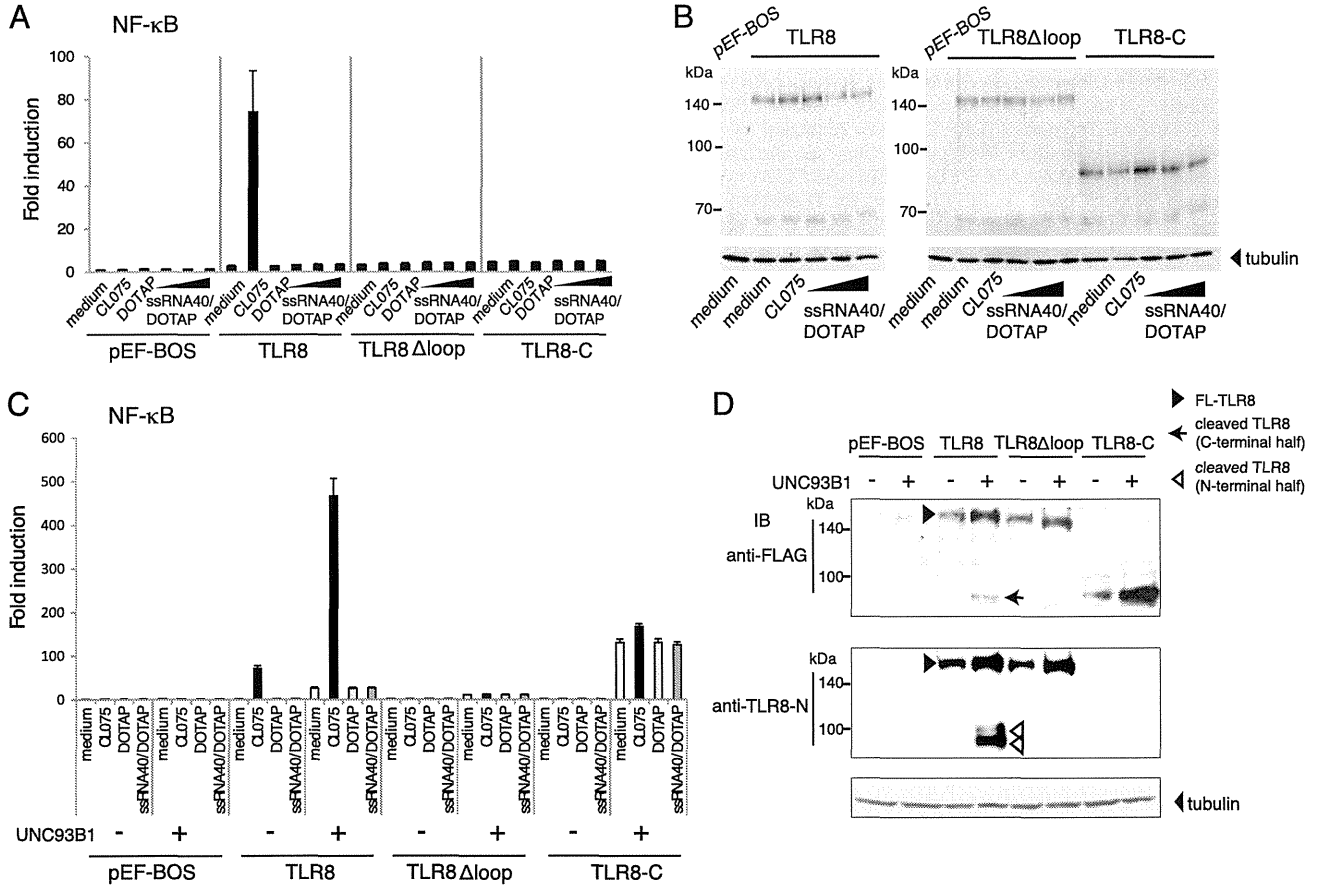

FIGURE 1. The flexible loop between LRR14 and LRR15 was required for CL075-induced TLR8-mediated NF-κB activation in HEK293 cells. (**A**) HEK293 cells were transiently transfected with vector alone or maximum amounts of C-terminal FLAG-tagged wild-type or mutant TLR8 plasmids (TLR8Δloop and TLR8-C), together with NF-κB–luciferase reporter plasmid and phRL-TK. Twenty-four hours after transfection, cells were stimulated with CL075 (2.5 μg/ml), DOTAP alone, or ssRNA40 complexed with DOTAP (2.5, 5, or 10 μg/ml) or were left untreated. Luciferase activity was measured 12 h after stimulation and expressed as fold induction relative to the activity of unstimulated cells. Representative data from three independent experiments, each performed in triplicate, are shown (mean ± SD). (**B**) Protein expression of wild-type and mutant TLR8 in HEK293 cells. Cell lysates prepared in (A) were subjected to SDS-PAGE (7.5%), followed by Western blotting with anti-FLAG mAb and anti–tubulin-α mAb. (**C**) Coexpression of UNC93B1 promoted CL075-induced TLR8-mediated NF-κB activation in HEK293 cells. HEK293 cells were transfected with the indicated plasmids together with NF-κB–luciferase reporter plasmid and phRL-TK. Cells were stimulated with 2.5 μg/ml CL075, DOTAP alone, or ssRNA40 complexed to DOTAP or were left untreated. Luciferase activity was measured 12 h after stimulation and expressed as fold induction relative to the activity of unstimulated cells. (**D**) Cell lysates prepared in (C) were subjected to SDS-PAGE (7.5%), followed by Western blotting with anti-FLAG mAb, anti–TLR8-N mAb, and anti–tubulin-α mAb. Filled arrowheads indicate full-length TLR8. Open arrowheads indicate N-terminal half of TLR8. Arrow indicates C-terminal half of TLR8.

truncated C-terminal half of TLR8 was unable to act as an RNA-sensing receptor. These results suggest that the loop region between LRR14 and LRR15 is crucial for ligand-induced TLR8-mediated signaling, as well as proteolytic processing of TLR8. UNC93B1 promoted proteolytic cleavage of TLR8 by facilitating ER exit of TLR8. In HEK293 cells transiently expressing TLR8, small amounts of cleaved TLR8 molecules appear to participate in the recognition of CL075 (Fig. 1A). Although the reason why ssRNA40 could not activate TLR8 in HEK293 cells ectopically expressing UNC93B1 is unclear, one possible interpretation is that oligomerization of multiple TLR8 molecules is required for ssRNA40-induced NF-κB activation. Notably, overexpressed wild-type and mutant TLR8, especially TLR8-C, activate NF-κB in a ligand-independent manner only when coexpressed with UNC93B1 (Fig. 1C, Supplemental Fig. 1), suggesting that transient overexpression and trafficking may allow TLR8–TIR domains to access each other, leading to activation of downstream signaling.

Cleavage of endogenous TLR8 in IFN-γ–treated THP-1 cells

THP-1 cells expressed TLR8 mRNA, which was upregulated by stimulation with IFN-γ (Fig. 2A) (40). To examine the structure of endogenous TLR8, we generated a pAb that recognizes the hTLR8 C-terminal peptides. The anti–TLR8-C pAb specifically recognized the full-length and C-terminal half of TLR8 but not N-terminal half of TLR8, hTLR7, or hTLR9 (Supplemental Fig. 2). In the IFN-γ–treated THP-1 cells, both full-length and C-terminal half of TLR8 proteins were detected by Western blotting with anti–TLR8-C Ab, indicating that endogenous TLR8 undergoes proteolytic processing (Fig. 2B). IFN-γ–treated THP-1 cells induced IL-12p40 mRNA expression in response to CL075, as well as ssRNA40, which was abolished by TLR8 knockdown (Fig. 2C).

Cleaved form of TLR8 is predominant in human primary monocytes and monocyte-derived macrophages

We investigated structural features of endogenous TLR8 in human primary cells, including monocytes and monocyte-derived macrophages. $CD14^+$ monocytes were successfully differentiated into macrophages after GM-CSF treatment for 6 d, in which the macrophage marker CD68 was greatly induced and the costimulatory molecule CD80 was upregulated by stimulation with CL075 (Supplemental Fig. 3). Immunoblotting with anti–TLR8-N and anti–TLR8-C Abs under reducing or nonreducing conditions clearly showed that TLR8 underwent proteolytic processing, and cleaved forms of TLR8 were predominant in monocytes and monocyte-derived macrophages (Fig. 3A). The TLR8 N-terminal halves consisted of two bands with a molecular mass ~100 and ~90 kDa. The C-terminal half was detected as a single band with a molecular mass ~90 kDa (Fig. 3A). None of the bands corresponding to TLR8 was observed in B cells, confirming the specificity of the TLR8 Abs used.

Upon stimulation with CL075 or ssRNA40 complexed to DOTAP, monocyte-derived macrophages produced a high level of IL-12p40 and some IL-6 and TNF-α, but their expression varied among different donors/individuals (Fig. 3B). Human monocyte-derived macrophages expressed low levels of TLR7; therefore, we examined whether the response to CL075 and ssRNA40 depended on TLR8 by knockdown analysis in macrophages. CL075- and ssRNA40-induced IL-12p40 mRNA expression was significantly reduced when TLR8 expression was knocked down at both the mRNA and protein levels (Fig. 3C). Notably, the expression and processing of TLR8 were mostly unaltered during differentiation from $CD14^+$ monocytes to macrophages, with the exception of day-1 monocytes after GM-CSF treatment: full-length TLR8 disappeared, and the lower band of TLR8-N was detected primarily (Fig. 4A). The response of TLR8 to ssRNA40 was unchanged during differentiation (Fig. 4B). Absence of full-length TLR8 at day 1 upon differentiation of monocytes with GM-CSF was observed consistently, irrelevant of the donor. These results suggest that the cleaved form of TLR8 is a functional receptor in human primary cells.

Both furin-like proprotein convertase and cathepsins are involved in stepwise processing of hTLR8

Two TLR8-Ns with different molecular masses were detected in monocyte and macrophage lysates; thus, we examined the proteases involved in TLR8 cleavage in human primary cells using protease inhibitors. Treatment of macrophages with z-FA-FMK, a cysteine protease inhibitor that blocks cathepsin proteolytic activity, failed to reduce both TLR8 cleavage and response to TLR8 agonists, probably because the cleaved form of TLR8 was abundant in macrophages (data not shown). When monocytes were differentiated into macrophages with GM-CSF in the presence of z-FA-FMK, an ~100-kDa upper band of TLR8-N accumulated from days 1 to 3, compared with DMSO-treated monocyte differentiation that mainly contained the lower band of TLR8-N (Fig. 5A, *upper panels*). This suggests that the upper band of TLR8-N is

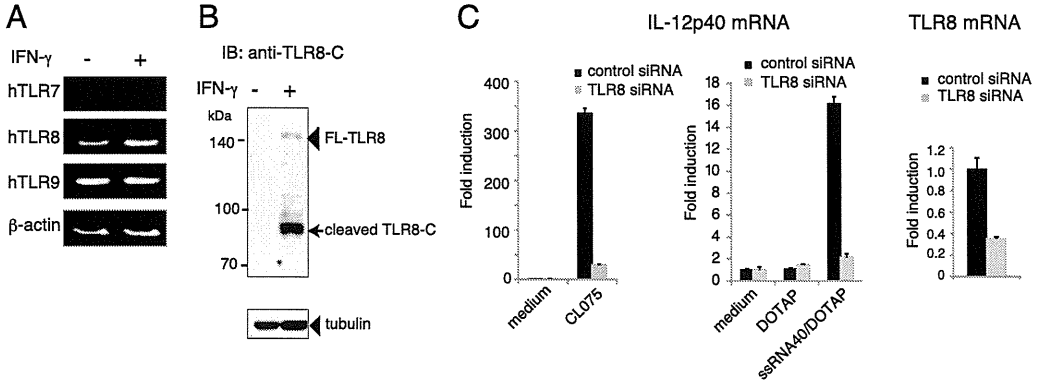

FIGURE 2. Human TLR8 underwent proteolytic processing in IFN-γ–treated THP-1 cells. (**A**) THP-1 cells (5×10^5/ml) were stimulated with 20 ng/ml IFN-γ or were left untreated for 15 h. Expression of TLR7, TLR8, and TLR9 mRNAs was analyzed by RT-PCR using specific primers (Supplemental Table I) (56). (**B**) Lysates of IFN-γ–treated or untreated THP-1 cells were subjected to SDS-PAGE, followed by Western blotting with anti–hTLR8-C pAb and anti–tubulin-α mAb. Arrowhead indicates full-length TLR8. Arrow indicates C-terminal half of TLR8. (**C**) Control or TLR8–knocked down IFN-γ–treated THP-1 cells (5×10^5/ml) were stimulated with medium alone, 2.5 μg/ml CL075, DOTAP alone, or 2.5 μg/ml ssRNA40 complexed to DOTAP. After 12 h, total RNA was extracted, and quantitative PCR was performed using primers for the IL-12p40 and TLR8 genes. Expression of genes was normalized to β-actin mRNA expression. Knockdown efficiency is shown (*right panel*). Representative data from two independent experiments are shown (mean ± SD).

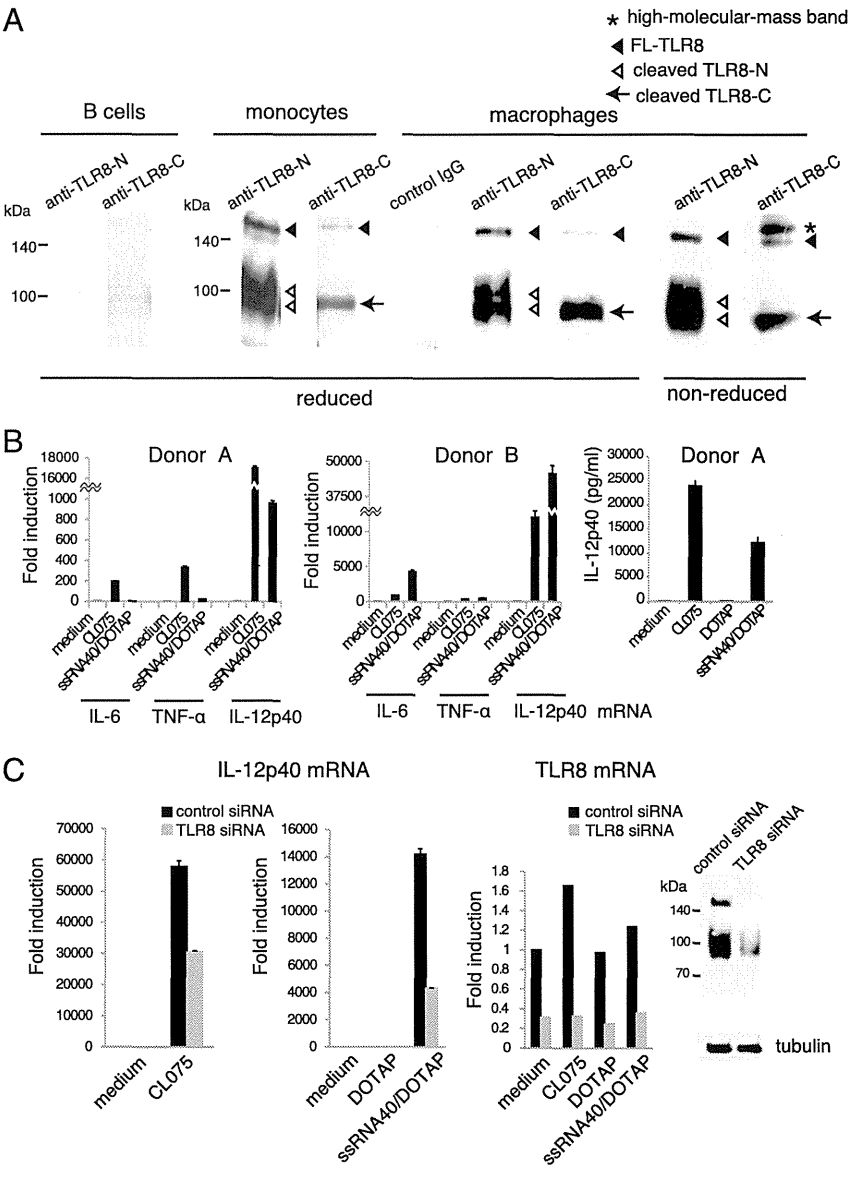

FIGURE 3. Cleaved form of TLR8 was predominant in human monocytes and monocyte-derived macrophages. (**A**) Lysates of human monocytes and monocyte-derived macrophages were subjected to SDS-PAGE under reducing or nonreducing conditions, followed by Western blotting with anti–TLR8-N mAb, anti–TLR8-C pAb, or control rabbit IgG. Lysates of B cells were used as cellular negative control. Filled arrowheads indicate full-length TLR8 (~150 kDa). Open arrowheads indicates N-terminal halves of TLR8 (~100 and ~90 kDa). Arrows indicate C-terminal half of TLR8 (90 kDa). Asterisk indicates high molecular mass band of TLR8. (**B**) Human monocyte-derived macrophages from different healthy donors were stimulated with the indicated ligands for 3 h, and IL-6, IL-12p40, and TNF-α transcripts were measured by quantitative PCR (*left* and *middle panels*). Protein levels of IL-12p40 in culture supernatants after 24 h of stimulation (donor A) were quantified using ELISA (*right panel*). (**C**) TLR8 is indispensable for ssRNA-induced cytokine production by human macrophages. Monocyte-derived macrophages (5×10^5/ml) were transfected with 30 pmol control or TLR8 siRNA. Forty-eight hours after transfection, cells were washed and stimulated with medium alone, 2.5 μg/ml CL075, DOTAP alone, or 2.5 μg/ml ssRNA40 complexed to DOTAP for 3 h, and IL-12p40 mRNA was measured by quantitative PCR. Knockdown of TLR8 mRNA and protein was confirmed by quantitative PCR and Western blotting with anti–TLR8-N mAb, respectively. Representative data from three independent experiments are shown (mean ± SD).

a premature form, and cysteine proteases, such as the cathepsin family, participate in further processing to generate the mature form of TLR8-N. Correlatively, when day-1 and day-2 monocytes were stimulated with CL075 or ssRNA40 complexed to DOTAP for 24 h, IL-12p40 production was decreased in z-FA-FMK–treated monocytes compared with DMSO-treated cells (Fig. 5A, *lower panel*). Considering that TLR7 was barely expressed in day- 1 to day-3 differentiated monocytes, involvement of TLR7 in CL075-induced IL-12p40 production is minimal, at best, under these experimental conditions. LPS-induced IL-12p40 production by these differentiated monocytes was unaltered in the presence of z-FA-FMK (data not shown).

A recent study demonstrated that furin-like proprotein convertase participates in processing of hTLR7 (30). We assessed the role of furin-like proprotein convertase in hTLR8 processing. Inhibition of furin-like proprotein convertase using DC1 reduced the response of macrophage TLR8 to CL075 and ssRNA40 but not to LPS (Fig. 5B). The cleaved TLR8-C and two TLR8-Ns, especially the upper band of TLR8-N, were reduced in DC1-treated macrophages compared with DMSO-treated cells (Fig. 5B, data not shown). Because a potential furin-like proprotein convertase–recognition site is present in the flexible loop between LRR14 and LRR15 of hTLR8, we made TLR8 mutant R467A/R470A/R472A/R473A in which the arginine residues in the potential furin-like proprotein convertase–recognition site in the flexible loop were substituted with alanine. This TLR8 mutant completely failed to undergo proteolytic processing when ectopically expressed in HEK293 cells, with or without UNC93B1, resulting in no activation of NF-κB in response to CL075 (Fig. 5C). These results indicate that furin-like proprotein convertase is indispensable for TLR8 cleavage at an initial step. Thus, both furin-like proprotein convertase and cathepsins are involved in stepwise processing of TLR8-N in human primary monocytes and macrophages.

N- and C-terminal halves of hTLR8 associate with each other and ssRNA40 binds to the cleaved/associated TLR8

To explore the association of the N- and C- terminal halves of TLR8, C-terminal FLAG-tagged wild-type and mutant hTLR8 were stably expressed in the mouse macrophage cell line RAW264.7. Wild-type TLR8, but not TLR8Δloop, underwent proteolytic processing in RAW cells, similar to an endogenous TLR8 in human macrophages (Fig. 6A). The N-terminal half of TLR8 coimmunoprecipitated with the C-terminal half of TLR8 under reducing and nonreducing conditions, suggesting that both the N- and

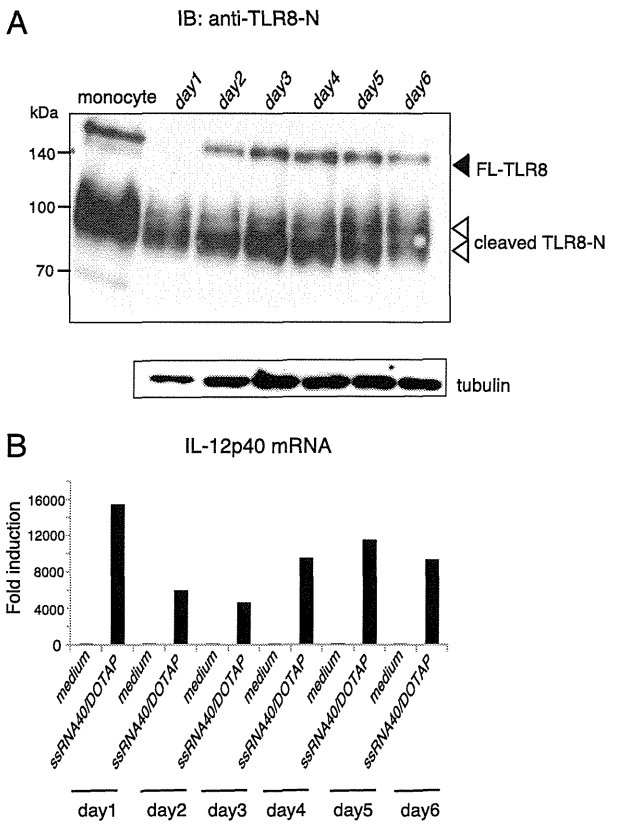

FIGURE 4. Expression and proteolytic processing of hTLR8 during differentiation from monocytes to macrophages. (**A**) $CD14^+$ human monocytes were cultured in medium containing GM-CSF for 1–6 d. TLR8 protein in differentiating cells was analyzed by western blotting with anti–TLR8-N mAb. Filled arrowhead indicates full-length TLR8. Open arrowheads indicate cleaved N-terminal halves of TLR8. (**B**) Response to ssRNA40 during differentiation from monocytes to macrophages. Differentiating cells were stimulated with 2.5 μg/ml ssRNA40 complexed to DOTAP for 3 h, and IL-12p40 transcript was measured by quantitative PCR. Representative data from more than three independent experiments are shown. In every experiment, full-length TLR8 was absent at day 1 upon differentiation of monocytes to macrophages after GM-CSF treatment.

C-terminal halves were noncovalently associated with each other in macrophages (Fig. 6B). We examined the interaction of ssRNA with TLR8 by pull-down assay using human macrophage lysates and biotinylated ssRNA40. After incubation of biotinylated ssRNA40 in the human macrophage lysates, ssRNA40–receptor complex was pulled down with avidin-Sepharose. Both the N- and C-terminal halves of TLR8 were pulled down, indicating that ssRNA40 bound to the cleaved/associated form of TLR8 (Fig. 6C).

Intracellular trafficking of hTLR8

TLR8 localizes to the ER and early endosome in primary human monocytes and HeLa cells transiently expressing hTLR8 (10). We examined the glycosylation of TLR8 protein in monocyte-derived macrophages with Endoglycosidase H, which hydrolyzes the high-mannose type *N*-glycans and *N*-glycosidase F that cleaves all types of asparagine-bound *N*-glycans. Deglycosylation analysis clearly showed that TLR8 was cleaved after passing through the Golgi, because most of the sugars on the cleaved TLR8-N were resistant to Endoglycosidase H and sensitive to *N*-glycosidase F (Fig. 7A). In contrast, N-linked sugars on full-length TLR8 were sensitive to Endoglycosidase H, indicating that an ~150-kDa band corresponding to full-length TLR8 was derived from the ER (Fig. 7A). The full-length TLR8 proteins accumulated in macrophages by brefeldin A treatment that disrupted the Golgi pathway (Fig. 7B).

Coexpression of UNC93B1 with TLR8 facilitated intracellular trafficking of TLR8 in HEK293 cells, resulting in accumulation of cleaved TLR8 (Fig. 1D). Confocal immunofluorescence analysis demonstrated that colocalization of TLR8 with p115 (Golgi-resident protein) was increased by UNC93B1 coexpression (Fig. 8A). TLR8 colocalized with MPR (late endosome marker protein), but not LysoTracker (lysosome marker), in UNC93B1-expressing cells (Fig. 8A). In human monocyte-derived macrophages, TLR8 colocalized with early endosome Ag 1 (early endosome marker protein), MPR, and calnexin (ER protein) but not with Lamp-1 (lysosome marker protein) (Fig. 8B). Taken together, these results indicated that TLR8 exits the ER, passes through the Golgi, and is targeted to early/late endosomes where the processing occurs.

Discussion

In the current study, we showed for the first time, to our knowledge, that proteolytic processing of TLR8 occurs in human primary cells, including monocytes and monocyte-derived macrophages, in a different manner from that of TLR7 and TLR9 cleavage. The insertion loop between LRR14 and LRR15 in TLR8 ECD is indispensable for cleavage and stepwise processing that occurs in the N-terminal fragment. Both furin-like proprotein convertase and cathepsins contribute to TLR8 cleavage in the early/late endosomes. Recent structural analysis of hTLR8 ECD–chemical ligand complex demonstrated that purified TLR8 ECD protein is cleaved at the loop region, and the N- and C-terminal halves remain associated, which contributes to ligand recognition and dimerization (39). Indeed, noncovalent association of the N-terminal half of TLR8 with the C-terminal half was detected by immunoprecipitation assay in RAW macrophages stably expressing hTLR8 (Fig. 6B). Furthermore, a pull-down assay revealed that ssRNA bound to the cleaved/associated form of TLR8 in human macrophages (Fig. 6C).

TLR8 belongs to the same subfamily as TLR7 and TLR9 (14, 15), but localization and signaling are quite different. We showed that hTLR8 localized to the ER and the early/late endosomes, but not to the lysosome, in monocytes and macrophages (Fig. 8B) (10), whereas mTLR7 and mTLR9 localized to the endolysosomes of macrophages and pDCs (8). The pH-dependent cathepsin family and AEP are involved in the stepwise processing of TLR7 and TLR9 at the C-terminal portion in mouse macrophages and DCs, although their contribution depends on cell type (24–29). In contrast, hTLR7 is processed at neutral pH, which is mediated with furin-like proprotein convertase (30). In the case of hTLR8, cathepsins mediate second-step processing of the N-terminal half, resulting in the generation of the mature form of the N-terminal half (Fig. 5A). Like hTLR7 processing, furin-like proprotein convertase is indispensable for TLR8 cleavage at an early step (Fig. 5B, 5C). Indeed, potential furin-like proprotein convertase–recognition sites are present in LRR14 and the flexible loop of hTLR8; one such site is located just before the N-terminus of the C-terminal ECD fragment (39). The TLR8 mutant R467A/R470A/R472A/R473A, in which arginine residues in the potential furin-like proprotein convertase–recognition site were substituted with alanine, was uncleaved when ectopically expressed in HEK293 cells and failed to transmit signals upon stimulation with CL075 (Fig. 5C). Although a putative asparagine cleavage site for AEP is found in the flexible loop of hTLR8 compared with that of mTLR7/9 (27), this site is located within the TLR8-C sequence, suggesting that AEP does not participate in TLR8 cleavage. Thus, proteases involved in processing of TLR7, TLR8, and TLR9 appear to be different and might depend on the localization of receptors and species- and cell type–specific protease distribution.

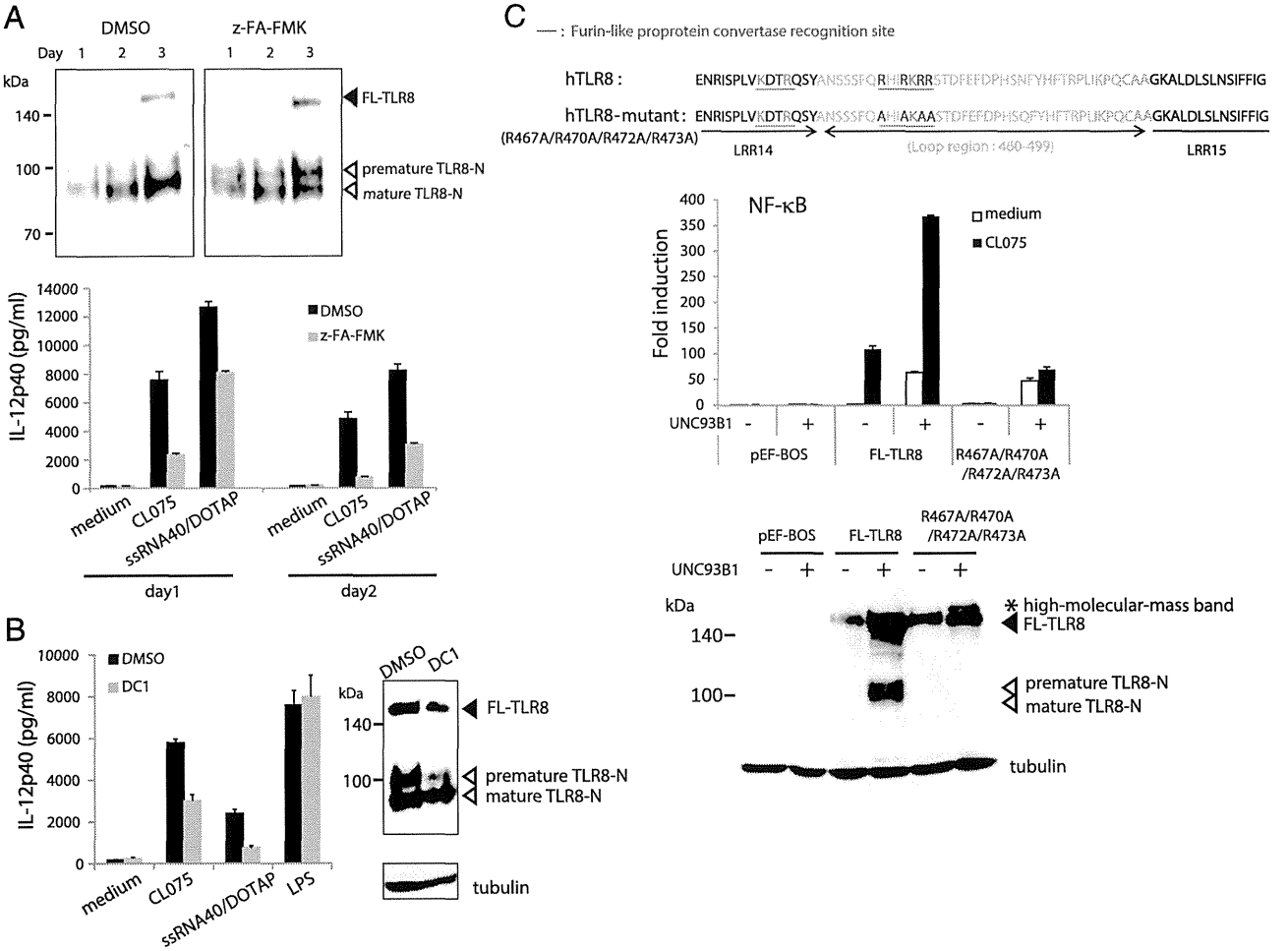

FIGURE 5. Furin-like proprotein convertases and cathepsins are involved in stepwise processing of hTLR8. (**A**) Monocytes were treated with GM-CSF in the presence or absence of 10 μM z-FA-FMK for up to 3 d. At day 1, day 2, and day 3, cells were lysed, and lysates were subjected to SDS-PAGE under reducing conditions, followed by Western blotting with anti–TLR8-N mAb (*upper panels*). The day-1 and day-2 monocytes were stimulated with medium alone, CL075 (2.5 μg/ml), or ssRNA40 complexed to DOTAP (2.5 μg/ml) for 24 h. IL-12p40 in the culture supernatants was measured using ELISA (*lower panel*). (**B**) Monocyte-derived macrophages were pretreated with 20 μM DC1 for 4 h and then stimulated with medium alone, CL075 (2.5 μg/ml), ssRNA40 complexed to DOTAP (2.5 μg/ml), or LPS (1 μg/ml) for 24 h. IL-12p40 in the culture supernatants was measured using ELISA (*left panel*). Lysates of DC1-treated macrophages were analyzed by Western blotting with anti–TLR8-N mAb and anti–tubulin-α mAb (*right panel*). (**C**) The potential furin-like proprotein convertase–recognition sites in LRR14 and insertion loop of hTLR8 (*upper panel*). Furin-like proprotein covertase–recognition site is R/K-Xn-R/K (X, any amino acid residue; n = 0, 2, 4, or 6). HEK293 cells were transfected with empty vector, wild-type TLR8 or R467A/R470A/R472A/R473A TLR8 mutant plasmid together with NF-κB–luciferase reporter plasmid and phRL-TK (*middle panel*). Cells were stimulated with 2.5 μg/ml CL075 or were left untreated. Luciferase activity was measured 12 h after stimulation and expressed as fold induction relative to the activity of unstimulated cells (mean ± SD). Cell lysates prepared in the reporter assay (medium stimulation) were subjected to SDS-PAGE (7.5%), followed by Western blotting with anti–TLR8-N mAb and anti–tubulin-α mAb (*bottom panel*). Closed arrowhead indicates full-length TLR8. Open arrowheads indicate premature and mature TLR8-N. Asterisk indicates high molecular mass band of TLR8. Representative data from two independent experiments are shown.

In freshly isolated human monocytes, cathepsins B and L are distributed in endosomes rather than lysosomes, and their sp. act. is observed in endosomal, but not in lysosomal, fractions (41). In addition, both cathepsins are expressed in HEK293 and THP-1 cells, whereas cathepsin S is expressed in THP-1 cells but not in HEK293 cells (K. Iwano, A. Watanabe, and M. Matsumoto, unpublished data). Considering the endosomal, but not lysosomal, localization of hTLR8, stepwise processing of hTLR8 by furin-like proprotein convertase and members of the cathepsin family, such as cathepsins B and L, might occur in early/late endosomes.

UNC93B1 mediates ER exit of TLR8, resulting in the accumulation of cleaved TLR8 in HEK293 cells (Fig. 1D). Notably, the TLR8-activating ability was different between CL075 and ssRNA40 in HEK293 cells transiently expressing TLR8 (Fig. 1). Structural analysis of unliganded and liganded TLR8 ECD revealed that cleaved/associated TLR8 dimerizes without ligand, and ligand binding to both N- and C-terminal halves induces structural reorganization of the TLR8 dimer (39). Mutagenesis analysis showed that interaction sites of TLR8 ECD with ssRNA appear to differ from those with chemical ligands. Oligomerization of TLR8 dimer might be required for ssRNA-induced signaling like dsRNA-induced TLR3-mediated signaling (42). In HEK293 cells, a small number of cleaved/associated TLR8 molecules is unable to induce signals to activate NF-κB in response to ssRNA40. In any case, our cellular analysis indicates that cleaved/associated TLR8 is responsible for recognition of both chemical ligands and ssRNA, and it induces innate immune responses in human primary cells.

Recent reports showed that dsRNA-sensing TLR3 undergoes cathepsin-mediated cleavage in a cell type–dependent manner (43–45). In addition, TLR3 recognizes incomplete stem structures formed in ssRNA (46). The nucleic acid–sensing TLRs respond to

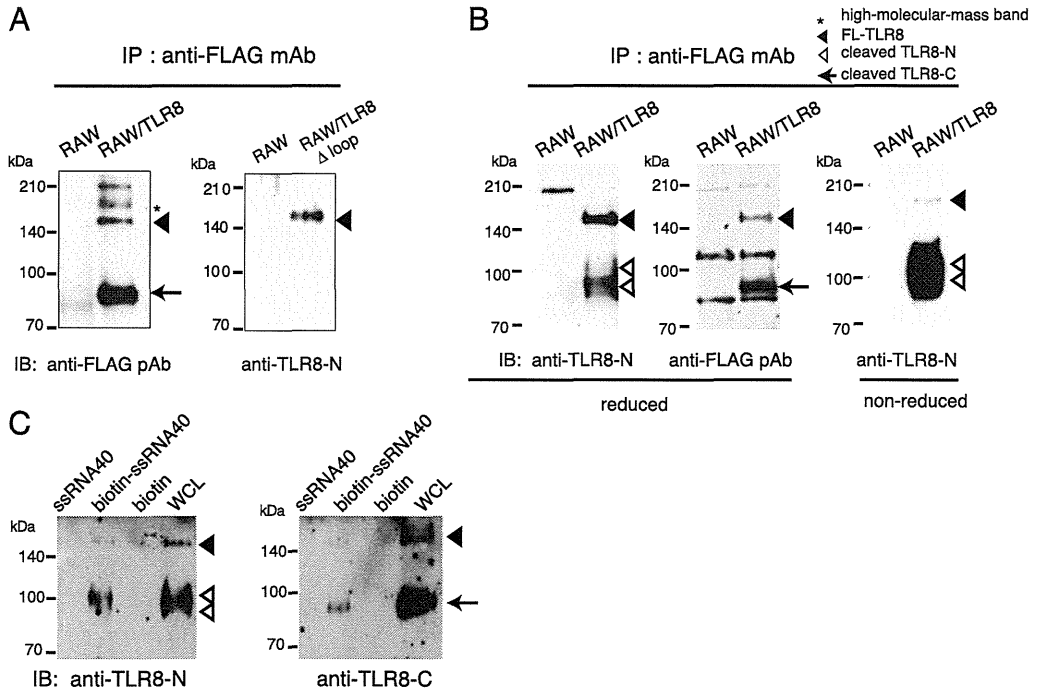

FIGURE 6. The N-terminal half of TLR8 is noncovalently associated with the C-terminal half. (**A**) Immunoblot analysis of RAW264.7 cells stably expressing C-terminal FLAG-tagged hTLR8 or hTLR8Δloop mutant. Cell lysates were immunoprecipitated (IP) with anti-FLAG mAb. The immunoprecipitates were resolved by SDS-PAGE, followed by immunoblotting (IB) with anti-FLAG pAb or anti–TLR8-N mAb. (**B**) Cell lysates of RAW264.7 cells stably expressing C-terminal FLAG-tagged hTLR8 were immunoprecipitated with anti-FLAG mAb. The immunoprecipitates were resolved by SDS-PAGE under reducing and nonreducing conditions, followed by immunoblotting with anti–TLR8-N mAb. The blot was reprobed with anti-FLAG pAb (*middle panel*). The ~210-kDa band is a nonspecific band observed in RAW cells. (**C**) ssRNA40 bound to the cleaved TLR8. Lysates of human macrophages were incubated with ssRNA40 (2.5 μg), biotinylated ssRNA40 (2.5 μg), or biotin (0.145 μg) or were left untreated for 1 h at 4°C and pulled down with streptavidin-Sepharose. Samples were analyzed by SDS-PAGE under reducing conditions, followed by immunoblotting with anti–TLR8-N mAb and anti–TLR8-C pAb.

microbial nucleic acid, as well as to endogenous self nucleic acids, in a sequence-independent, but motif-dependent, manner. Hence, the cleaved/associated form of receptors might be beneficial for recognition of nucleic acids with different nucleotide sequences and structures (47).

The role of TLR8 in antiviral immunity in humans remains unknown. In the case of HIV infection, TLR8 signaling appears to benefit HIV replication (48), but another study demonstrated an anti-HIV function for TLR8 (49). TLR8 expressed in neutrophils mediates neutrophil extracellular trap formation in HIV-1 infection via recognition of viral nucleic acids, which is useful for HIV-1 elimination (50). In addition, TLR8-mediated IL-12p70 production by monocytes polarizes naive $CD4^+$ T cells into Th1 cells that mediate cellular immunity (51). Thus, TLR8 triggers important antimicrobial signals in distinctive cells that express TLR8 but not other nucleic acid–sensing TLRs.

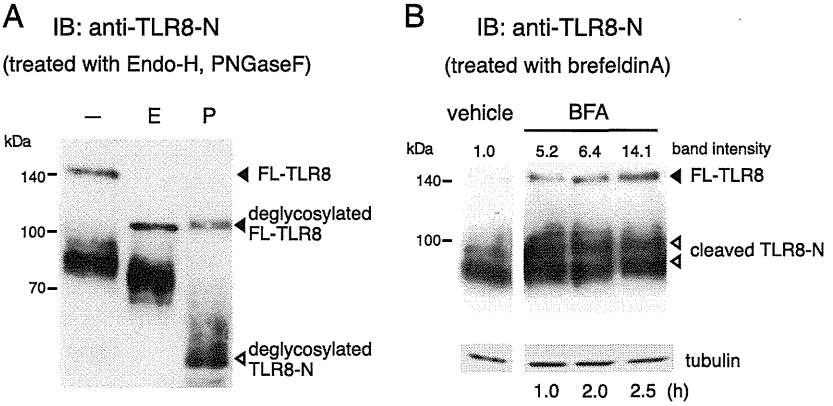

FIGURE 7. Cleaved TLR8 was generated after traveling through the Golgi. (**A**) Immunoblot (IB) analysis of monocyte-derived macrophage lysates (5×10^5) incubated with 1 μl Endoglycosidase H (E) or 2 μl *N*-glycosidase F (P) for 30 min at 37°C. Anti–TLR8-N mAb was used to detect full-length and cleaved TLR8. (**B**) Accumulation of full-length TLR8 by treatment of human macrophages with brefeldin A. Human macrophages were treated with brefeldin A (2 μg/ml), a reagent that disrupts the Golgi, or vehicle for the indicated lengths of time. Cell lysates were separated by SDS-PAGE under reducing conditions, followed by immunoblotting with anti–TLR8-N mAb. The band intensity of FL-TLR8 was quantified using National Institutes of Health ImageJ software and normalized to that of tubulin. Results are expressed as fold intensity relative to the intensity of vehicle-treated cells.

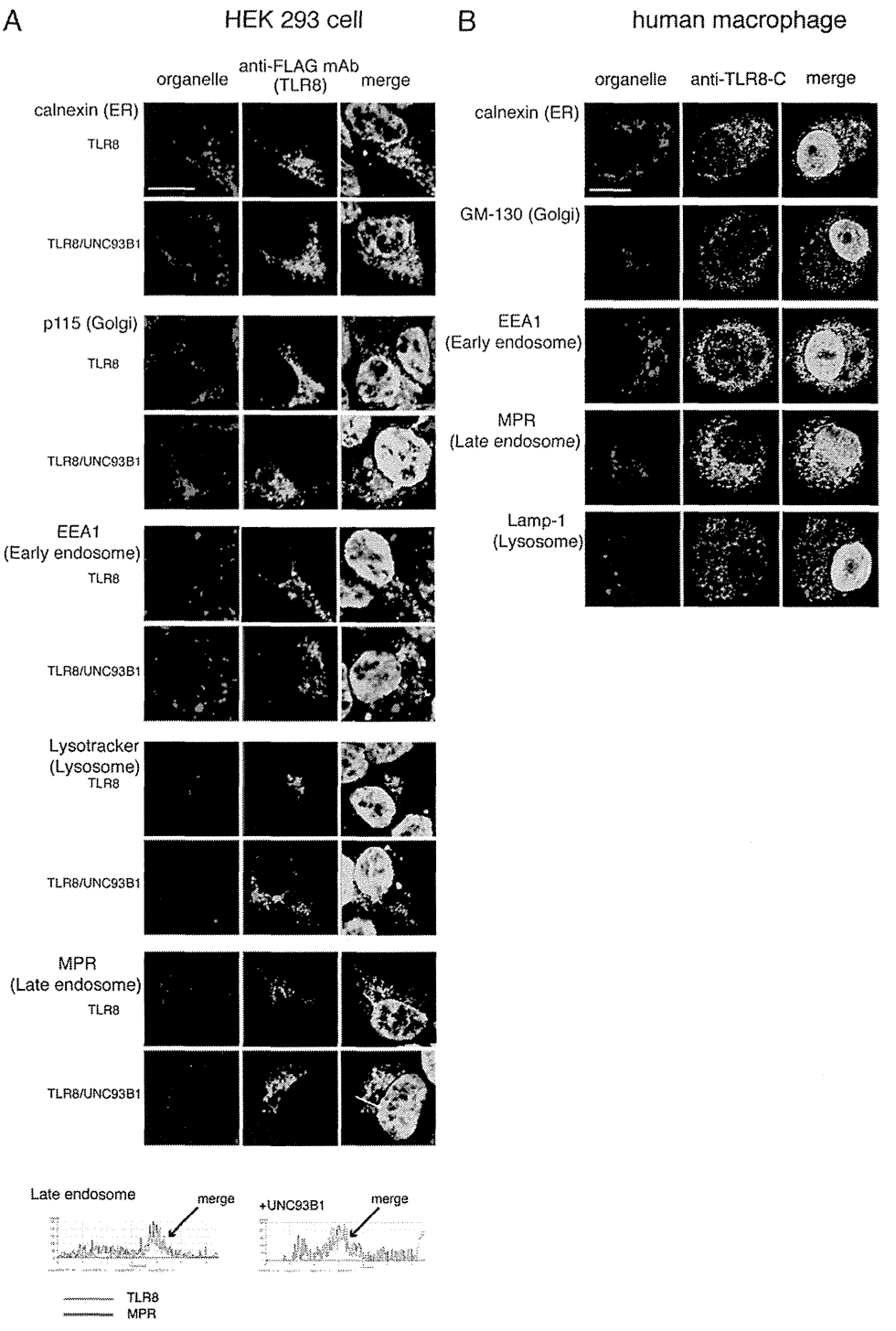

FIGURE 8. TLR8 localized to the early/late endosomes in human macrophages. (**A**) UNC93B1 facilitated intracellular trafficking of TLR8. HEK293 cells expressing FLAG-tagged hTLR8, with or without UNC93B1, were fixed, permeabilized, and stained with anti-FLAG mAb and the indicated pAbs against organelle marker proteins, followed by Alexa Fluor 488–labeled or Alexa Fluor 568–labeled secondary Ab. Red, organelle markers; green, TLR8; blue, DAPI-stained nuclei. Scale bar, 10 μm. Graphs display the measured fluorescence intensity along the white line in the merged panels of MPR and TLR8 with or without UNC93B1. (**B**) Subcellular localization of endogenous TLR8 in monocyte-derived macrophages. Macrophages were fixed, permeabilized, and stained with anti–TLR8-C pAb and the indicated mouse mAbs against organelle marker proteins, followed by Alexa Fluor 488–labeled or Alexa Fluor 568–labeled secondary Ab. Red, organelle markers; green, TLR8; blue, DAPI-stained nuclei. Scale bar, 10 μm.

TLR7 and TLR9 are closely associated with autoimmune disorders because of their expression in B cells and pDCs (52, 53). The relationship between TLR8 and autoimmune disorders was suggested in a TLR8-knockout mouse study that showed a pivotal role for mTLR8 in the regulation of TLR7 expression and prevention of spontaneous autoimmunity (54). In addition, a recent study using hTLR8-transgenic mice clearly demonstrated the connection between TLR8 and autoimmune inflammation (55). TLR8 was shown to induce proinflammatory cytokine production in response to microRNA within exosomes from tumor cells (38). In view of the unique expression profile and signaling skewed toward NF-κB activation, TLR8 might be involved in the development of inflammatory disorders in a distinct manner. Identification of endogenous and exogenous TLR8 ligands and their recognition mechanisms are important for a full understanding of the role of TLR8 in innate immunity and protection against undesirable inflammation and autoimmune responses.

Acknowledgments

We thank our laboratory members for valuable discussions. We also thank M. Nakai, R. Takemura, K. Mugikura, Y. Takeda, A. Maruyama, and K. Takashima for preparing blood cells. We also thank Dr. K. Miyake, Dr. S. Akira, and Dr. S. Nagata for providing the plasmids.

Disclosures

The authors have no financial conflicts of interest.

References

1. Medzhitov, R., and C. A. Janeway, Jr. 1997. Innate immunity: the virtues of a nonclonal system of recognition. *Cell* 91: 295–298.
2. Akira, S., S. Uematsu, and O. Takeuchi. 2006. Pathogen recognition and innate immunity. *Cell* 124: 783–801.
3. Barton, G. M., and J. C. Kagan. 2009. A cell biological view of Toll-like receptor function: regulation through compartmentalization. *Nat. Rev. Immunol.* 9: 535–542.
4. Matsumoto, M., K. Funami, M. Tanabe, H. Oshiumi, M. Shingai, Y. Seto, A. Yamamoto, and T. Seya. 2003. Subcellular localization of Toll-like receptor 3 in human dendritic cells. *J. Immunol.* 171: 3154–3162.
5. Latz, E., A. Schoenemeyer, A. Visintin, K. A. Fitzgerald, B. G. Monks, C. F. Knetter, E. Lien, N. J. Nilsen, T. Espevik, and D. T. Golenbock. 2004. TLR9 signals after translocating from the ER to CpG DNA in the lysosome. *Nat. Immunol.* 5: 190–198.
6. Tabeta, K., K. Hoebe, E. M. Janssen, X. Du, P. Georgel, K. Crozat, S. Mudd, N. Mann, S. Sovath, J. Goode, et al. 2006. The Unc93b1 mutation 3d disrupts exogenous antigen presentation and signaling via Toll-like receptors 3, 7 and 9. *Nat. Immunol.* 7: 156–164.
7. Brinkmann, M. M., E. Spooner, K. Hoebe, B. Beutler, H. L. Ploegh, and Y. M. Kim. 2007. The interaction between the ER membrane protein UNC93B and TLR3, 7, and 9 is crucial for TLR signaling. *J. Cell Biol.* 177: 265–275.
8. Kim, Y. M., M. M. Brinkmann, M. E. Paquet, and H. L. Ploegh. 2008. UNC93B1 delivers nucleotide-sensing toll-like receptors to endolysosomes. *Nature* 452: 234–238.
9. Fukui, R., S. Saitoh, F. Matsumoto, H. Kozuka-Hata, M. Oyama, K. Tabeta, B. Beutler, and K. Miyake. 2009. Unc93B1 biases Toll-like receptor responses to nucleic acid in dendritic cells toward DNA- but against RNA-sensing. *J. Exp. Med.* 206: 1339–1350.
10. Itoh, H., M. Tatematsu, A. Watanabe, K. Iwano, K. Funami, T. Seya, and M. Matsumoto. 2011. UNC93B1 physically associates with human TLR8 and regulates TLR8-mediated signaling. *PLoS ONE* 6: e28500.
11. Funami, K., M. Matsumoto, H. Oshiumi, T. Akazawa, A. Yamamoto, and T. Seya. 2004. The cytoplasmic 'linker region' in Toll-like receptor 3 controls receptor localization and signaling. *Int. Immunol.* 16: 1143–1154.
12. Nishiya, T., E. Kajita, S. Miwa, and A. L. Defranco. 2005. TLR3 and TLR7 are targeted to the same intracellular compartments by distinct regulatory elements. *J. Biol. Chem.* 280: 37107–37117.
13. Barton, G. M., J. C. Kagan, and R. Medzhitov. 2006. Intracellular localization of Toll-like receptor 9 prevents recognition of self DNA but facilitates access to viral DNA. *Nat. Immunol.* 7: 49–56.
14. Chuang, T.-H., and R. J. Ulevitch. 2000. Cloning and characterization of a sub-family of human toll-like receptors: hTLR7, hTLR8 and hTLR9. *Eur. Cytokine Netw.* 11: 372–378.
15. Du, X., A. Poltorak, Y. Wei, and B. Beutler. 2000. Three novel mammalian toll-like receptors: gene structure, expression, and evolution. *Eur. Cytokine Netw.* 11: 362–371.
16. Bell, J. K., G. E. D. Mullen, C. A. Leifer, A. Mazzoni, D. R. Davies, and D. M. Segal. 2003. Leucine-rich repeats and pathogen recognition in Toll-like receptors. *Trends Immunol.* 24: 528–533.
17. Latz, E., A. Verma, A. Visintin, M. Gong, C. M. Sirois, D. C. Klein, B. G. Monks, C. J. McKnight, M. S. Lamphier, W. P. Duprex, et al. 2007. Ligand-induced conformational changes allosterically activate Toll-like receptor 9. *Nat. Immunol.* 8: 772–779.
18. Hemmi, H., T. Kaisho, O. Takeuchi, S. Sato, H. Sanjo, K. Hoshino, T. Horiuchi, H. Tomizawa, K. Takeda, and S. Akira. 2002. Small anti-viral compounds activate immune cells via the TLR7 MyD88-dependent signaling pathway. *Nat. Immunol.* 3: 196–200.
19. Jurk, M., F. Heil, J. Vollmer, C. Schetter, A. M. Krieg, H. Wagner, G. Lipford, and S. Bauer. 2002. Human TLR7 or TLR8 independently confer responsiveness to the antiviral compound R-848. *Nat. Immunol.* 3: 499.
20. Heil, F., H. Hemmi, H. Hochrein, F. Ampenberger, C. Kirschning, S. Akira, G. Lipford, H. Wagner, and S. Bauer. 2004. Species-specific recognition of single-stranded RNA via toll-like receptor 7 and 8. *Science* 303: 1526–1529.
21. Diebold, S. S., T. Kaisho, H. Hemmi, S. Akira, and C. Reis e Sousa. 2004. Innate antiviral responses by means of TLR7-mediated recognition of single-stranded RNA. *Science* 303: 1529–1531.
22. Hemmi, H., O. Takeuchi, T. Kawai, T. Kaisho, S. Sato, H. Sanjo, M. Matsumoto, K. Hoshino, H. Wagner, K. Takeda, and S. Akira. 2000. A Toll-like receptor recognizes bacterial DNA. *Nature* 408: 740–745.
23. Krieg, A. M. 2002. CpG motifs in bacterial DNA and their immune effects. *Annu. Rev. Immunol.* 20: 709–760.
24. Matsumoto, F., S. Saitoh, R. Fukui, T. Kobayashi, N. Tanimura, K. Konno, Y. Kusumoto, S. Akashi-Takamura, and K. Miyake. 2008. Cathepsins are required for Toll-like receptor 9 responses. *Biochem. Biophys. Res. Commun.* 367: 693–699.
25. Ewald, S. E., B. L. Lee, L. Lau, K. E. Wickliffe, G. P. Shi, H. A. Chapman, and G. M. Barton. 2008. The ectodomain of Toll-like receptor 9 is cleaved to generate a functional receptor. *Nature* 456: 658–662.
26. Park, B., M. M. Brinkmann, E. Spooner, C. C. Lee, Y. M. Kim, and H. L. Ploegh. 2008. Proteolytic cleavage in an endolysosomal compartment is required for activation of Toll-like receptor 9. *Nat. Immunol.* 9: 1407–1414.
27. Sepulveda, F. E., S. Maschalidi, R. Colisson, L. Heslop, C. Ghirelli, E. Sakka, A. M. Lennon-Duménil, S. Amigorena, L. Cabanie, and B. Manoury. 2009. Critical role for asparagine endopeptidase in endocytic Toll-like receptor signaling in dendritic cells. *Immunity* 31: 737–748.
28. Ewald, S. E., A. Engel, J. Lee, M. Wang, M. Bogyo, and G. M. Barton. 2011. Nucleic acid recognition by Toll-like receptors is coupled to stepwise processing by cathepsins and asparagine endopeptidase. *J. Exp. Med.* 208: 643–651.
29. Maschalidi, S., S. Hässler, F. Blanc, F. E. Sepulveda, M. Tohme, M. Chignard, P. van Endert, M. Si-Tahar, D. Descamps, and B. Manoury. 2012. Asparagine endopeptidase controls anti-influenza virus immune responses through TLR7 activation. *PLoS Pathog.* 8: e1002841.
30. Hipp, M. M., D. Shepherd, U. Gileadi, M. C. Aichinger, B. M. Kessler, M. J. Edelmann, R. Essalmani, N. G. Seidah, C. Reis e Sousa, and V. Cerundolo. 2013. Processing of human toll-like receptor 7 by furin-like proprotein convertases is required for its accumulation and activity in endosomes. *Immunity* 39: 711–721.
31. Kanno, A., C. Yamamoto, M. Onji, R. Fukui, S. Saitoh, Y. Motoi, T. Shibata, F. Matsumoto, T. Muta, and K. Miyake. 2013. Essential role for Toll-like receptor 7 (TLR7)-unique cysteines in an intramolecular disulfide bond, proteolytic cleavage and RNA sensing. *Int. Immunol.* 25: 413–422.
32. Onji, M., A. Kanno, S. Saitoh, R. Fukui, Y. Motoi, T. Shibata, F. Matsumoto, A. Lamichhane, S. Sato, H. Kiyono, et al. 2013. An essential role for the N-terminal fragment of Toll-like receptor 9 in DNA sensing. *Nat. Commun.* 4: 1949.
33. Hornung, V., S. Rothenfusser, S. Britsch, A. Krug, B. Jahrsdörfer, T. Giese, S. Endres, and G. Hartmann. 2002. Quantitative expression of toll-like receptor 1-10 mRNA in cellular subsets of human peripheral blood mononuclear cells and sensitivity to CpG oligodeoxynucleotides. *J. Immunol.* 168: 4531–4537.
34. Peng, G., Z. Guo, Y. Kiniwa, K. S. Voo, W. Peng, T. Fu, D. Y. Wang, Y. Li, H. Y. Wang, and R. F. Wang. 2005. Toll-like receptor 8-mediated reversal of CD4+ regulatory T cell function. *Science* 309: 1380–1384.
35. Janke, M., J. Poth, V. Wimmenauer, T. Giese, C. Coch, W. Barchet, M. Schlee, and G. Hartmann. 2009. Selective and direct activation of human neutrophils but not eosinophils by Toll-like receptor 8. *J. Allergy Clin. Immunol.* 123: 1026–1033.
36. Jongbloed, S. L., A. J. Kassianos, K. J. McDonald, G. J. Clark, X. Ju, C. E. Angel, C. J. Chen, P. R. Dunbar, R. B. Wadley, V. Jeet, et al. 2010. Human CD141+ (BDCA-3)+ dendritic cells (DCs) represent a unique myeloid DC subset that cross-presents necrotic cell antigens. *J. Exp. Med.* 207: 1247–1260.
37. Sarvestani, S. T., B. R. Williams, and M. P. Gantier. 2012. Human Toll-like receptor 8 can be cool too: implications for foreign RNA sensing. *J. Interferon Cytokine Res.* 32: 350–361.
38. Fabbri, M., A. Paone, F. Calore, R. Galli, E. Gaudio, R. Santhanam, F. Lovat, P. Fadda, C. Mao, G. J. Nuovo, et al. 2012. MicroRNAs bind to Toll-like receptors to induce prometastatic inflammatory response. *Proc. Natl. Acad. Sci. USA* 109: E2110–E2116.
39. Tanji, H., U. Ohto, T. Shibata, K. Miyake, and T. Shimizu. 2013. Structural reorganization of the Toll-like receptor 8 dimer induced by agonistic ligands. *Science* 339: 1426–1429.
40. Zarember, K. A., and P. J. Godowski. 2002. Tissue expression of human Toll-like receptors and differential regulation of Toll-like receptor mRNAs in leukocytes in response to microbes, their products, and cytokines. *J. Immunol.* 168: 554–561.
41. Schmid, H., R. Sauerbrei, G. Schwarz, E. Weber, H. Kalbacher, and C. Driessen. 2002. Modulation of the endosomal and lysosomal distribution of cathepsins B, L and S in human monocytes/macrophages. *Biol. Chem.* 383: 1277–1283.
42. Matsumoto, M., and T. Seya. 2008. TLR3: interferon induction by double-stranded RNA including poly(I:C). *Adv. Drug Deliv. Rev.* 60: 805–812.
43. Garcia-Cattaneo, A., F. X. Gobert, M. Müller, F. Toscano, M. Flores, A. Lescure, E. Del Nery, and P. Benaroch. 2012. Cleavage of Toll-like receptor 3 by cathepsins B and H is essential for signaling. *Proc. Natl. Acad. Sci. USA* 109: 9053–9058.
44. Qi, R., D. Singh, and C. C. Kao. 2012. Proteolytic processing regulates Toll-like receptor 3 stability and endosomal localization. *J. Biol. Chem.* 287: 32617–32629.
45. Toscano, F., Y. Estornes, F. Virard, A. Garcia-Cattaneo, A. Pierrot, B. Vanbervliet, M. Bonnin, M. J. Ciancanelli, S. Y. Zhang, K. Funami, et al. 2013. Cleaved/associated TLR3 represents the primary form of the signaling receptor. *J. Immunol.* 190: 764–773.
46. Tatematsu, M., F. Nishikawa, T. Seya, and M. Matsumoto. 2013. Toll-like receptor 3 recognizes incomplete stem structures in single-stranded viral RNA. *Nat. Commun.* 4: 1833.
47. Li, Y., I. C. Berke, and Y. Modis. 2012. DNA binding to proteolytically activated TLR9 is sequence-independent and enhanced by DNA curvature. *EMBO J.* 31: 919–931.
48. Gringhuis, S. I., M. van der Vlist, L. M. van den Berg, J. den Dunnen, M. Litjens, and T. B. Geijtenbeek. 2010. HIV-1 exploits innate signaling by TLR8 and DC-SIGN for productive infection of dendritic cells. *Nat. Immunol.* 11: 419–426.
49. Han, X., X. Li, S. C. Yue, A. Anandaiah, F. Hashem, P. S. Reinach, H. Koziel, and S. D. Tachado. 2012. Epigenetic regulation of tumor necrosis factor α (TNFα) release in human macrophages by HIV-1 single-stranded RNA (ssRNA) is dependent on TLR8 signaling. *J. Biol. Chem.* 287: 13778–13786.
50. Saitoh, T., J. Komano, Y. Saitoh, T. Misawa, M. Takahama, T. Kozaki, T. Uehata, H. Iwasaki, H. Omori, S. Yamaoka, et al. 2012. Neutrophil extracellular traps mediate a host defense response to human immunodeficiency virus-1. *Cell Host Microbe* 12: 109–116.
51. Ablasser, A., H. Poeck, D. Anz, M. Berger, M. Schlee, S. Kim, C. Bourquin, N. Goutagny, Z. Jiang, K. A. Fitzgerald, et al. 2009. Selection of molecular structure and delivery of RNA oligonucleotides to activate TLR7 versus TLR8 and to induce high amounts of IL-12p70 in primary human monocytes. *J. Immunol.* 182: 6824–6833.

52. Marshak-Rothstein, A. 2006. Toll-like receptors in systemic autoimmune disease. *Nat. Rev. Immunol.* 6: 823–835.
53. Krieg, A. M., and J. Vollmer. 2007. Toll-like receptors 7, 8, and 9: linking innate immunity to autoimmunity. *Immunol. Rev.* 220: 251–269.
54. Demaria, O., P. P. Pagni, S. Traub, A. de Gassart, N. Branzk, A. J. Murphy, D. M. Valenzuela, G. D. Yancopoulos, R. A. Flavell, and L. Alexopoulou. 2010. TLR8 deficiency leads to autoimmunity in mice. *J. Clin. Invest.* 120: 3651–3662.
55. Guiducci, C., M. Gong, A.-M. Cepika, Z. Xu, C. Tripodo, L. Bennett, C. Crain, P. Quartier, J. J. Cush, V. Pascual, et al. 2013. RNA recognition by human TLR8 can lead to autoimmune inflammation. *J. Exp. Med.* 210: 2903–2919.
56. Kokkinopoulos, I., W. J. Jordan, and M. A. Ritter. 2005. Toll-like receptor mRNA expression patterns in human dendritic cells and monocytes. *Molec. Immunol.* 42: 957–968.

Supplementary Table SI

PCR primers used in this study

hTLR7-Fw	5'-TTACCTGGATGGAAACCAGC-3'
hTLR7-Re	5'-GCAGAATTTACCATCCCCA-3'
hTLR8-Fw	5'-CAGAATAGCAGGCGTAACACATCA3'
hTLR8-Re	5'-AATGTCACAGGTGCATTCAAAGGG-3'
hTLR9-Fw	5'-TTATGGACTTCCTGCTGGAGGTGC-3'
hTLR9-Re	5'-CTGCGTTTTGTCGAAGACCA-3'
β-actin-Fw	5'-ATCTGGCACCACACCTTCTACAATGAGCTGCG-3'
β-actin-Re	5'-CGTCATACTCCTGCTTGCTGATCCACATCTGC-3'

qPCR primers used in this study

hTLR8-Fw	5'-GAGAGCCGAGACAAAAACGTTC-3'
hTLR8-Re	5'-TGTCGATGATGGCCAATCC-3'
TNF-α-Fw	5'-TCTTCTCGAACCCCGAGTGA-3'
TNF-α-Re	5'-AGCTGCCCCTCAGCTTGA-3'
IL-6-Fw	5'-CTCCAGGAGCCCAGCTATGA-3'
IL-6-Re	5'-CCCAGGGAGAAGGCAACTG-3'
IL-12p40-Fw	5'-CTGTGCCCTGCAGTTAGGTTC-3'
IL-12p40-Re	5'-TCCACTTTTCCTCCAAATTTTCA-3'
β-actin-Fw	5'-CCTGGCACCCAGCACAAT-3'
β-actin-Re	5'-GCCGATCCACACGGAGTACT-3'

Supplementary Figure S1. Ishii et al.

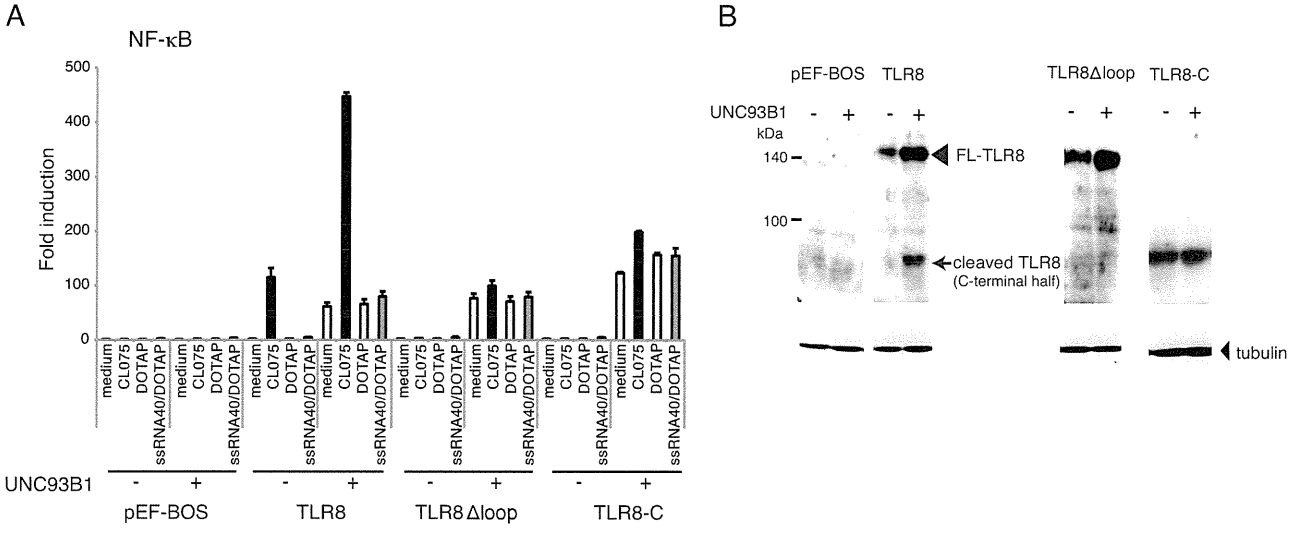

Supplementary Figure S1. UNC93B1 promoted CL075-induced TLR8-mediated NF-κB activation in HEK293 cells.

A, HEK293 cells were transiently transfected with maximum amounts of C-terminal FLAG-tagged wild-type or mutant TLR8 plasmids (TLR8Δloop and TLR8-C) (56 ng), UNC93B1 plasmid (14 ng) or vector alone together with NF-κB–luciferase reporter plasmid and phRL-TK. Twenty-four hours after transfection, cells were stimulated with CL075 (2.5 μg/ml), DOTAP alone, ssRNA40 complexed with DOTAP (2.5 μg/ml) or left untreated. Luciferase activity was measured 12 h after stimulation and expressed as fold induction relative to the activity of unstimulated cells. Representative data from two independent experiments, each performed in triplicate, are shown (mean ± SD).

B, Protein expression of wild-type and mutant TLR8 in HEK293 cells. Cell lysates prepared in A (medium) were subjected to SDS-PAGE (7.5%) followed by western blotting with anti-FLAG mAb and anti-tubulin α mAb.

Supplementary Figure S2. Ishii et al.

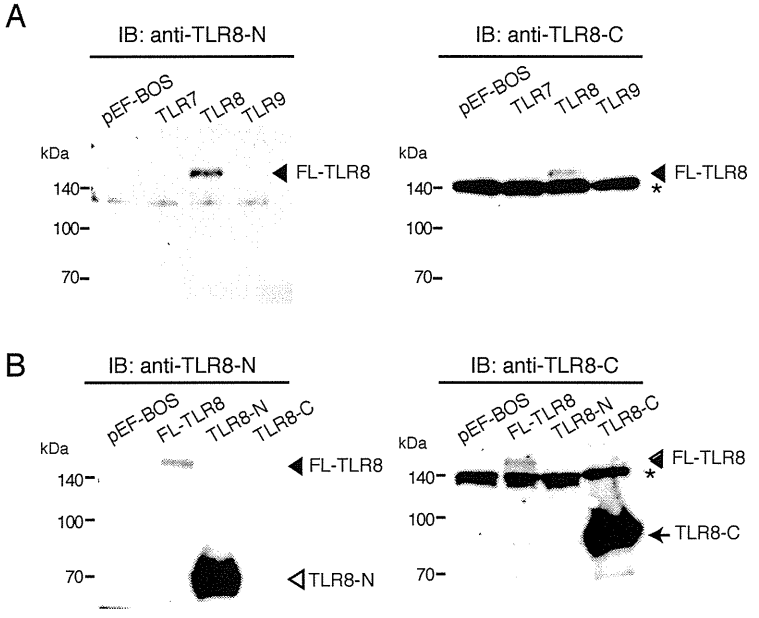

Supplementary Figure S2. Characterization of anti-human TLR8-C pAb.
A, B, HEK293FT cells were transfected with the indicated plasmids. Twenty-four hours after transfection, cells were lysed and subjected to SDS-PAGE followed by immunoblotting with anti-TLR8-N mAb and anti-TLR8-C pAb. Asterisk indicates non-specific bands. TLR8-N represents a truncated mutant form of TLR8 that consists of LRR-NT and LRR1–14.

Supplementary Figure S3. Ishii et al.

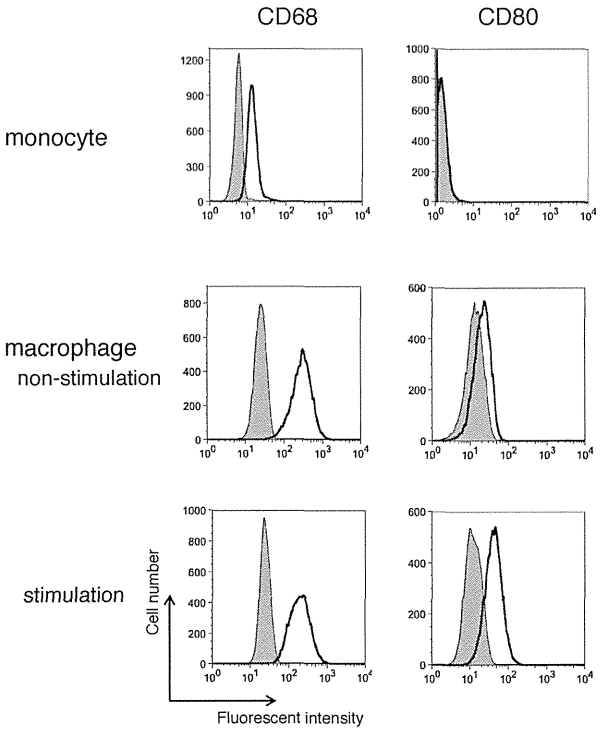

Supplementary Figure S3. Flow cytometric analysis of CD68 and CD80 expression in human monocytes and monocyte-derived macrophages. Monocytes and monocyte-derived macrophages stimulated with 2.5 μg/ml CL075 for 24 h or left untreated were stained with FITC anti-human CD68 mAb or PE anti-human CD80 mAb.
Shaded histograms represent cells labeled with isotype-matched control Ab.

PLOS ONE

Suppression of La Antigen Exerts Potential Antiviral Effects against Hepatitis A Virus

Xia Jiang[1☯], Tatsuo Kanda[1*☯], Shuang Wu[1], Shingo Nakamoto[2], Kengo Saito[2], Hiroshi Shirasawa[2], Tomoko Kiyohara[3], Koji Ishii[3], Takaji Wakita[3], Hiroaki Okamoto[4], Osamu Yokosuka[1]

1 Department of Gastroenterology and Nephrology, Chiba University, Graduate School of Medicine, Chiba, Japan, **2** Department of Molecular Virology, Chiba University, Graduate School of Medicine, Chiba, Japan, **3** Department of Virology II, National Institute of Infectious Diseases, Musashimurayama, Japan, **4** Division of Virology, Department of Infection and Immunity, Jichi Medical University School of Medicine, Shimotsuke, Japan

Abstract

Background: Despite the development and availability of hepatitis A virus (HAV) vaccine, HAV infection is still a major cause of acute hepatitis that occasionally leads to fatal liver disease. HAV internal ribosomal entry-site (IRES) is one of the attractive targets of antiviral agents against HAV. The aim of the present study is to evaluate the impact of La, one of the cellular proteins, on HAV IRES-mediated translation and HAV replication.

Methods and Findings: We investigated the therapeutic feasibility of siRNAs specific for cellular cofactors for HAV IRES-mediated translation in cell culture. It was revealed that siRNA against La could inhibit HAV IRES activities as well as HAV subgenomic replication. We also found that the Janus kinase (JAK) inhibitors SD-1029 and AG490, which reduce La expression, could inhibit HAV IRES activities as well as HAV replication.

Conclusions: Inhibition of La by siRNAs and chemical agents could lead to the efficient inhibition of HAV IRES-mediated translation and HAV replication in cell culture models. La might play important roles in HAV replication and is being exploited as one of the therapeutic targets of host-targeting antivirals.

Citation: Jiang X, Kanda T, Wu S, Nakamoto S, Saito K, et al. (2014) Suppression of La Antigen Exerts Potential Antiviral Effects against Hepatitis A Virus. PLoS ONE 9(7): e101993. doi:10.1371/journal.pone.0101993

Editor: Ratna B. Ray, Saint Louis University, United States of America

Received May 20, 2014; **Accepted** June 12, 2014; **Published** July 7, 2014

Data Availability: The authors confirm that all data underlying the findings are fully available without restriction. All relevant data are within the paper and its Supporting Information files.

Funding: This work was supported by grants from the Ministry of Health, Labour and Welfare of Japan (H24-Hepatitis-General-002)(OY). The funders had no role in study design, data collection and analysis, decision to publish, or preparation of the manuscript.

Competing Interests: The authors have declared that no competing interests exist.

* Email: kandat@aol.com

☯ These authors contributed equally to this work.

Introduction

Hepatitis A virus (HAV) is a non-enveloped single-stranded RNA virus, with ~7.6 kb positive-sense genome. The genome includes 5′ non-translated region (5′NTR), one open reading frame encoding structural (VP4, VP2, VP3, VP4 and 2A) and non-structural proteins (2B, 2C, 3A, 3B, 3C and 3D), and 3′NTR [1]. HAV genome translation could be initiated by cap-independent mechanism through HAV internal ribosomal entry-site (IRES) with a pyrimidine-rich tract, which is located at the down-stream part of 5′NTR [2]. HAV is still a major cause of acute hepatitis [3,4]. Although acute liver failure due to HAV is not common, it is still occasionally fatal [5], despite HAV vaccine having become available [6–8]. This emphasizes the importance of the development of antiviral agents against HAV.

In general, two distinct classes of antiviral agents, direct-acting antivirals (DAAs) and host-targeting antivirals (HTAs), exist [9]. Several groups have reported DAAs against HAV, such as inhibitors of HAV 3C cysteine proteinase, which is essential for viral replication and infectivity [10–15]. Small interfering RNAs against HAV genome are also varieties of DAAs [16–18]. Several broad-target HTAs, examples of which include interferon-α, interferon-β, interferon-λ1 and amantadine, have been developed and tested against HAV [2,19–25]. These compounds could inhibit HAV IRES-dependent translation as well as HAV replication [2,21,22]. HTAs of the targeted group are more precise in that they act on key host enzymes or cellular factors that are required for the viral lifecycle [9].

Our previous studies suggested that several siRNAs against HAV 5′NTR suppress HAV translation as well as HAV replication [17]. The nucleotide sequences of 5′NTR are one of the most conserved in HAV genomes [8,26]. These facts suggest that HAV IRES is one of the attractive targets of antiviral agents against HAV. It has been reported that several cellular proteins such as autoantigen La [27], glyceraldehyde-3-phosphate dehydrogenase (GAPDH) [28,29], polypyrimidine tract-binding protein (PTB/hnRNPI) [29–31], poly(C) binding protein 2 (PCBP2/hnRNP-E2) [32], polyadenylate-binding protein-1 (PABP) [33], eukaryotic translation initiation factor 4E (eIF4E) [34] and eukaryotic translation initiation factor 4E (eIF4G) [33,35,36] could interact with HAV IRES *in vitro* or *in vivo*, and could be associated with HAV replication.

Human La protein is predominantly localized in the nucleus and is associated with RNA metabolism [37]. It has been reported that La was associated with U1 RNA [38], telomerase RNA [39], 5′NTR of poliovirus [27], hepatitis C virus (HCV) [40] and GRP78/Bip [41]. La could interfere with IRES-mediated translation.

In the present study, we investigated the therapeutic feasibility of siRNAs specific for these putative cellular cofactors for HAV IRES-mediated translation. It was revealed that siRNA against La (siRNA-La) could inhibit HAV IRES activities as well as HAV subgenomic replication. We also found that JAK inhibitors SD-1029 and AG490, which inhibit La expression, could inhibit HAV IRES activities as well as HAV replication. The present study demonstrated the proof-of-concept for the inhibition of La as a method for suppressing HAV replication.

Results

Effects of silencing of cellular factors on HAV IRES-mediated translation

Although the exact mechanisms are not fully understood, it has been reported that HAV IRES could interact with various endogenous genes [27–34], suggesting important roles of these proteins in HAV IRES-mediated translation and HAV replication. La, GAPDH, PTB and PCBP2 have been shown to bind to HAV IRES domains IIIb and V [23], IIIa [28], I-IIIb [30] and I-IIIb [32], respectively. PABP, eIF4E and eIF4G also interact with HAV IRES [33–36]. To determine whether each siRNA against these factors had a specific siRNA effect, knockdown of these molecules was validated by Western blotting, respectively (Figure 1A–1G). To examine the effects of the knockdown of these genes on HAV IRES-mediated translation, Huh7 cells were cotransfected with each siRNA, and pSV40-HAV-IRES, which contains SV40 promoter, renilla luciferase (Rluc) and nt. 139–854 of HAV sequence fused firefly luciferase (Fluc) gene [2]. After 48 h transfection, the cell lysates were analyzed for HAV IRES activities (Fluc/Rluc) as previously described (Figure 1H) [17,21]. Compared with the HAV IRES activity in Huh7 cells transfected with control siRNA (siRNA-control) (100%), that transfected with siRNA-La was 39%, but those of the others were not inhibited (Figure 1H). These results provide further evidence of La being a potential cofactor for HAV IRES activity, indicating the possible usefulness of siRNA-La against HAV infection.

Effects of silencing of La on HAV subgenomic replication

Next, we examined the effect of the silencing of La on HAV subgenomic replication [42] (Figure 2). To test luciferase activity due to translation or translation and replication, we introduced a replication-competent HAV replicon (pT7-18f-LUC) and a replication-incompetent HAV replicon (pT7-18f-LUC mut) into HuhT7 cells [21,42], with or without amantadine treatment, which is effective for suppressing HAV replication [2,21]. Reporter assays were performed 24 h, 48 h or 72 h after transfection. Relative luciferase activities of pT7-18f-LUC co-transfected with siRNA-control or siRNA-La, respectively, were 100% or 15.4% at 24 h, 100% or 28.7% at 48 h, and 100% or 21.7% at 72 h after transfection (Figure 2A). On the other hand, those of pT7-18f-LUC mut cotransfected with siRNA-control or siRNA-La, respectively, were 94% or 3.7% at 24 h, 63.8% or 7.9% at 48 h, and 54.2% or 2.9% at 72 h after transfection (Figure 2A). Because the luciferase values of pT7-18f-LUC or pT7-18f-LUC mut were due to translation with replication or translation without replication, respectively [21,42], it was confirmed that siRNA-La might suppress HAV IRES-mediated translation. The effects of siRNA-La also enhanced the amantadine induced-suppression of HAV subgenomic replication (Figure 2B).

JAK inhibitors AG490 and SD-1029 could suppress La expression

Because it was reported that La expression is dependent on $JAK2^{V617F}$ in murine pro B Ba/F3-EPOR-derived cell line [42], the effects of two JAK2 inhibitors, AG490 and SD-1029, on La expression were examined. Initially, we evaluated the cytotoxicity of AG490 and SD-1029 on African green kidney GL37 cells by 3-(4,5-dimethylthiazol-2-yl)-5-(3-carboxymethoxyphenyl)-2-(4-sulfophenyl)-2H-tetrazolium, inner salt (MTS) assay. AG490 concentration in a range of 100–10,000 nM and SD-1029 concentration in a range of 100–5,000 nM were not toxic in 48-h incubation (Figure 3A, 3B). With these concentrations, we tested the effects of AG490 and SD-1029 on La expression in GL37 cells, which supports HAV replication [21]. The results of Western blotting showed that La expression was decreased in a concentration-dependent manner with AG490 (Figure 3C) and SD-1029 (Figure 3D). These data prompted us to examine whether these drugs had an inhibitory effect on HAV IRES-mediated translation or HAV replication.

Effects of AG490 and SD-1029 on HAV IRES-mediated translation

COS7 cells stably expressing pSV40-HAV-IRES (COS7-HAV-IRES cells) were generated. To evaluate HAV IRES activity, after COS7 cells were cotransfected with pSV40-HAV IRES and pCXN2, and cultured in the presence of 500 μg/mL G418 for 3 weeks, COS7-HAV-IRES cells were established, making it easy to evaluate HAV IRES activity (Figure 4A). Treatment of these cells with AG490 resulted in the inhibition of HAV IRES activities (100%, 94%, 99%, 93%, 71% and 70% at 0, 100, 500, 1,000, 5,000 and 10,000 nM AG490, respectively) (Figure 4B). Treatment of these cells with SD-1029 resulted in the inhibition of HAV IRES activities (100%, 95%, 96%, 85%, 42% and 21% at 0, 100, 500, 1,000, 5,000 and 10,000 nM SD-1029, respectively) (Figure 4C).

Effects of AG490 and SD-1029 on HAV replication

We established GL37 stably expressing both short hairpin (sh)RNA-La (GL37-shLa cells) and control shRNA (GL37-shC cells) after GL37 cells were cotransfected with plasmid shRNA-La and plasmid shRNA-control, respectively, and cultured in the presence of puromycin. We examined whether shRNA-La could inhibit the replication of HAV HA11-1299 genotype IIIA strain in these GL37-derived cell lines. Western blotting analysis demonstrated that knockdown of La was validated in GL37-shLa cells, compared to GL37-shC cells (Figure 5A). As shown in Figure 5B, HAV RNA levels were 6.07×10^5 copies/μg cellular RNA (92%) in GL37-shLa cells, in comparison with 6.63×10^5 copies/μg cellular RNA (100%) in GL37-shC cells after 72 h of HAV infection at a multiplicity of infection (MOI) of 0.1.

Next, we investigated whether AG490 or SD-1029 could inhibit the replication of HAV HA11-1299 genotype IIIA strain in GL37 cells. Cells were treated with AG490 or SD-1029 for 24 h, infected with HAV HA11-1299 genotype IIIA strain at MOI of 0.1, and washed with PBS 7 h later. After 96 h of HAV infection, cellular RNA was extracted, and HAV RNA levels were determined using real-time RT-PCR. As shown in Figure 5C, HAV RNA levels were 5.27×10^4, 5.46×10^4 or 2.58×10^4 copies/μg of cellular RNA (63%, 65% or 31%) in GL37 treated with 100, 1,000 or

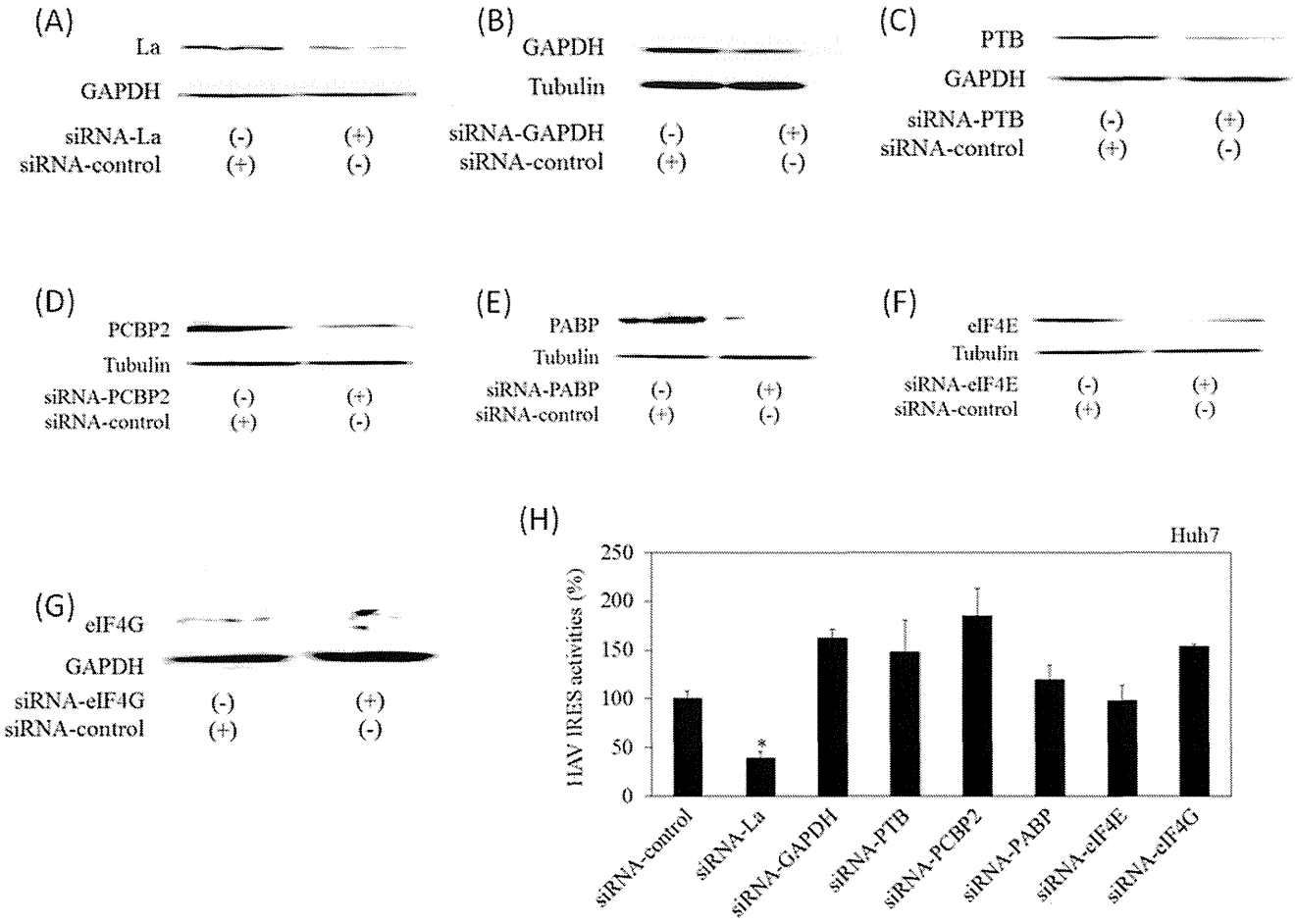

Figure 1. Knockdown of La inhibits hepatitis A virus (HAV) internal ribosomal entry site (IRES) activities. Effects of siRNAs on endogenous gene expression in Huh7 (A–G). Approximately 0.5×10^6 cells were transfected with 100 nM siRNA against La (siRNA-La), glyceraldehyde-3-phosphate dehydrogenase (GAPDH) (siRNA-GAPDH), polypyrimidine tract-binding protein (PTB/hnRNPI) (siRNA-PTB), poly(C) binding protein 2 (PCBP2/hnRNP-E2) (siRNA-PCBP2), polyadenylate-binding protein-1 (PABP) (siRNA-PABP), eukaryotic translation initiation factor 4E (eIF4E) (siRNA-eIF4E), eukaryotic translation initiation factor 4E (eIF4G) (siRNA-eIF4G) or control siRNA (siRNA-control). Protein expression was determined by Western blotting using each specific antibody. GAPDH or tubulin was used as control. (A) La, (B) GAPDH, (C) PTB/hnRNPI, (D) PCBP2, (E) PABP, (F) eIF4E, and (G) eIF4G expressions are shown. (H) Effects of each siRNA on the HAV IRES activities. Huh7 cells were cotransfected with 0.3 μg pSV40-HAV-IRES [2] with each siRNA at 100 nM. Cells were harvested 48 h post-transfection and luciferase activities were measured. Activities of HAV IRES were calculated as previously described [17,21]. Data are expressed as mean ± SD. *$P<0.05$ vs. Huh7 cells transfected with (siRNA-control).*
doi:10.1371/journal.pone.0101993.g001

10,000 nM AG490, respectively, in comparison with 8.35×10^4 copies/μg of cellular RNA (100%) in GL37 without any treatment after 96 h of HAV infection at MOI of 0.1. As shown in Figure 5D, HAV RNA levels were 4.26×10^4 or 4.12×10^4 copies/μg cellular RNA (51% or 49%) in GL37 treated with 100 or 1,000 nM SD-1029, respectively, in comparison with that in GL37 without any treatment after 96 h of HAV infection at a MOI of 0.1. ELISA analysis of tissue culture-adapted HAV KRM003 genotype IIIB strain in GL37 cells [21] also showed mild inhibition of viral propagation with 500–1,000 nM AG490 but not with SD-1029 at 48 h post-infection (data not shown).

Discussion

In the present study, we examined the effects of the knockdown of La in cell lines infected with HAV. We observed the inhibition of HAV replication by sh-La. We also observed that inhibitors of La, AG490 and SD-1029, induced the suppression of HAV genotype IIIA replication. Of course, HAV vaccine has already been developed. Although patients with acute hepatitis A are not usually treated with antiviral drugs, there are occasionally patients with severe acute hepatitis A such as fatal acute liver failure. To our knowledge, ours is the first study to report that a reduction of La can suppress HAV replication in cell culture.

It has been reported that down-regulation of La was induced by (-)-epigallocatechin gallate, iron chelator deferxamine and JAK inhibitor AZD1480 [43–45]. Ferric ammonium citrate up-regulates La expression [45]. It was reported that HBSC-11, an inhibitor of La, has an anti-HBV activity in which HBSC-11 may be mediated by a reduction in La levels [46]. Because we did not observe any effects of (-)-epigallocatechin gallate or ferric ammonium citrate on La expression in our experiments (data not shown), we chose JAK inhibitors in the present study. Our study suggested that anti-HAV activity of AG490 and SD-1029 should also be mediated by a reduction of La. It is possible that La inhibitors could be useful as antiviral drugs.

The use of 1,000 nM of AG490 and SD-1029 reduced La expression in GL37 cells (Figure 3C, 3D). However, there were no effects on HAV IRES activities up to this concentration in COS7-

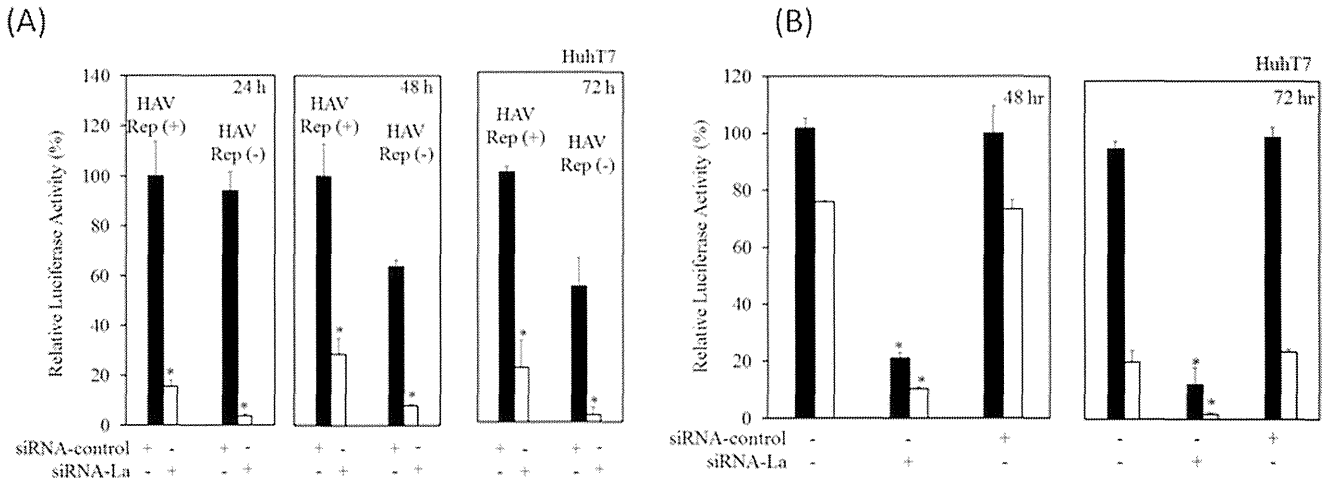

Figure 2. Knockdown of La inhibits hepatitis A virus (HAV) subgenomic replication. (A) Effects of siRNA against La (siRNA-La) on the HAV replication-competent replicon pT7-18f-LUC [HAV Rep (+)] or replication-incompetent replicon pT7-18f-LUCmut [HAV Rep (−)] replication. Approximately 0.5×10^6 HuhT7 cells were cotransfected with 0.3 μg pT7-18f-LUC/pT7-18f-LUCmut [42] and 100 nM siRNA against La (siRNA-La)/control siRNA (siRNA-control). After 24 h (left), 48 h (middle) or 72 h (right), cell lysates were collected and luciferase activities were measured. (B) Effects of siRNA against La (siRNA-La) with or without amantadine on the HAV subgenomic replication-competent replicon pT7-18f-LUC. Approximately 0.5×10^6 HuhT7 cells were cotransfected with 0.3 μg pT7-18f-LUC and 50 nM siRNA against La (siRNA-La)/control siRNA (siRNA-control). After 24 h transfection, cells were treated with 5 μg/mL amantadine (white column) or without (black column). After 48 h (left) or 72 h (right) transfection, cell lysates were collected and luciferase activities were measured. Data are expressed as mean ± SD. *$P<0.05$.
doi:10.1371/journal.pone.0101993.g002

HAV-IRES cells (Figure 4B, 4C). These discrepancies might be a result of these two different cell lines, or this might be one of the points needing improvement in COS7-HAV-IRES cells.

Although AZD1480 was an inhibitor of JAK1 and JAK2 [46], AG490 is a tyrosine kinase inhibitor of JAK2, JAK3, epidermal growth factor (EGFR) and v-erb-b2 avian erythroblastic leukemia viral oncogene homolog 2 (Neu) [47,48], and JAK2 inhibitor III SD-1029 acts as a JAK2-selective inhibitor [49]. Of interest is that these three JAK inhibitors reduce cellular La expression (Figure 3C and 3D) [45]. HAV and HCV modulate the JAK/STAT signaling pathway [50,51]. Further studies will be needed at this stage, although several specific JAK inhibitors have been developed and

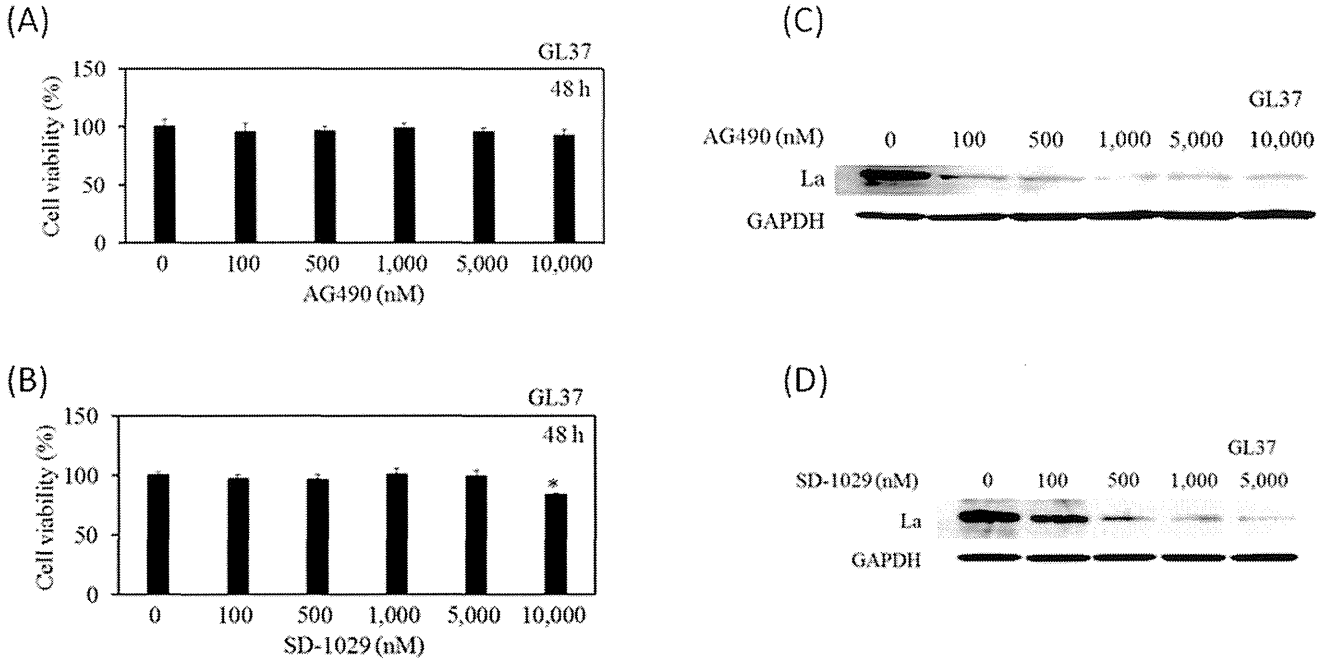

Figure 3. Effects of AG490 and SD-1029 on cell viability and La expression in GL37 cells. MTS assays of cells 48 h after treatment with AG490 (A) or SD-1029 (B) at indicated concentrations. Data are expressed as mean ± SD. Western blotting analysis. Approximately 1×10^5 cells were incubated in the presence of AG490 (C) or SD-1029 (D) at indicated concentrations. Twenty-four hours after treatment, cell lysates were analyzed for La and GAPDH expressions using specific antibodies. Data are expressed as mean ± SD. *$P<0.05$.
doi:10.1371/journal.pone.0101993.g003

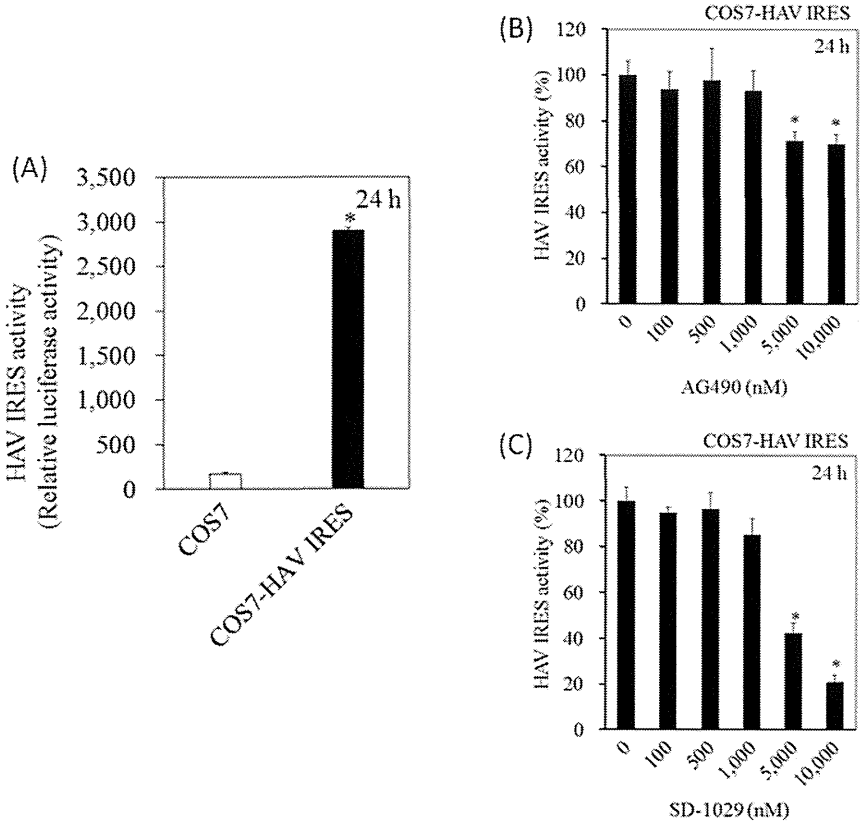

Figure 4. Effects of AG490 and SD-1029 on hepatitis A virus (HAV) internal ribosomal entry site (IRES) activities. (A) HAV IRES activities of COS7 cells stably expressing pSV40-HAV-IRES (COS7-HAV IRES cells). 0.5×10^5 cells were seeded, cell lysates were collected 24 h later, and luciferase assay was performed for determination of HAV IRES activities. (B) Effect of AG490 on HAV IRES activity in COS7-HAV IRES cells. (C) Effect of SD-1029 on HAV IRES activity in COS7-HAV IRES cells. The cells were cultured with AG490 or SD-1029 at the concentrations indicated, and reporter assay was performed after 24 h of treatment. Activities of HAV IRES were calculated as previously described [17,21]. Data are expressed as mean ± SD. *$P<0.05$.
doi:10.1371/journal.pone.0101993.g004

there are ongoing trials for the treatment of myeloproliferative neoplasms [52], allergic skin diseases [53] and rheumatoid arthritis [54].

HAV replicates in the cytoplasm of hepatocytes, although La exists predominantly in the nucleus [37]. Previous studies have suggested that La associates with IRES-mediated translation [27,40,41], and the present study also demonstrated that La plays a potential role in HAV IRES-mediated translation. Our result also showed that HAV IRES-mediated translation was helped by La, in contrast to the previous observation [27]. These differences might be related to the experimental system such as in vivo or in vitro, and cell lines. Although HAV RNA levels were reduced by 5.6×10^4 copies/μg cellular RNA when comparing GL37-shLa cells with GL37-shC cells (Figure 5B), it might be possible that other host factors are involved in suppressing HAV replication by JAK inhibitors. Further studies will be needed.

In the study field of HCV infection, the development of two distinct antiviral agents, DAAs and HTAs, could lead to higher sustained virological response rates via reductions of adverse events and treatment duration [9] compared to the former standard treatment [55]. The use of La inhibitor, one of the HTAs for HAV, alone or in combination with DAAs, might be beneficial for certain patients infected with HAV.

There are three HAV genotypes, I, II and III, of human origin [56]. The inhibitory effects of AG490 and SD-1029 on HAV subgenotype IIIA strain were observed by real-time PCR methods. But only weak inhibition of AG490 on HAV subgenotype IIIB was observed by ELISA methods. This may be related to the different methods of detection for HAV, that is, by RT-PCR or ELISA. There might also be differences among the different HAV subgenotypes, although HTAs have a high genetic barrier to resistance and a pan-genotypic antiviral activity [57]. Further studies on the exact mechanism of the association between La and HAV replication will be needed. In conclusion, inhibition of La by siRNAs and chemical agents could lead to the inhibition of HAV IRES-mediated translation and HAV replication in cell culture models. Our findings suggest that La plays important roles in HAV replication and should be exploited as one of the therapeutic targets.

Materials and Methods

Cells, virus and reagents

Human hepatoma cells (Huh7 and HuhT7, which stably express T7-RNA polymerase [42]) and African green monkey kidney cells (COS7 and GL37 [21,22,56,58]), were grown in Dulbecco's modified essential medium (DMEM, Sigma-Aldrich, St. Louis, MO, USA) containing 10% fetal bovine serum, 100 units/ml penicillin and 100 μg/ml streptomycin (Sigma) at 37°C in 5% CO_2. Huh7 and COS7 cells were purchased from JCRB cell bank, National Institute of Biomedical Innovation, Osaka, Japan. HAV subgenomic replicon was previously described [42]. Briefly, the structures of the competent HAV replicon (HAV) and incompetent HAV replicon (mut-HAV replicon) containing a

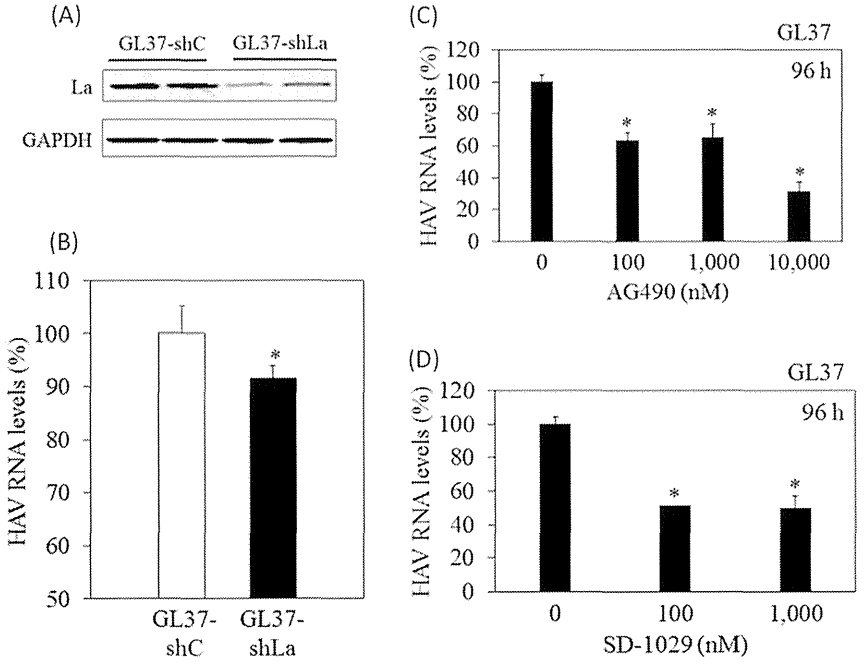

Figure 5. Antiviral activities of shRNA-La, AG490 and SD-1029 on hepatitis A virus (HAV) replication. (A) La protein expression in GL37 stably expressing shRNA-La (GL37-shLa cells) and GL37 stably expressing control shRNA (GL37-shC cells). Western blotting was performed with specific antibodies indicated. (B) Real-time PCR analysis of intracellular HAV RNA following HAV HA11-1299 genotype IIIA strain infection in GL37-shC or GL37-shLa cells. (C) Suppression of HAV infection in GL37 treated with AG490 at concentrations indicated. (D) Suppression of HAV infection in GL37 treated with SD-1029 at concentrations indicated. Cells were treated with AG490 or SD-1209 for 24 h, infected with HAV HA11-1299 genotype IIIA strain at MOI of 0.1, and washed with PBS 7 h later. After 96 h of HAV infection, cellular RNA was extracted, and HAV RNA levels were determined using real-time RT-PCR. Data are expressed as mean ± SD. *$P<0.05$.
doi:10.1371/journal.pone.0101993.g005

frame-shift mutation in polymerase 3D were reported [42]. These replicons also contain an open-reading frame of firefly luciferase. HAV HA11-1299 genotype IIIA strain and HAV KRM003 genotype IIIB strain [21] were also used. The simian virus (SV) 40 promoter plasmid pSV40-HAV IRES was used as reported previously [2,17]; it encodes in a bicistronic fashion the Renilla reniformis luciferase (Rluc), the hepatitis A virus internal ribosomal entry site (HAV IRES), followed by the firefly luciferase (Fluc). AG490 (Calbiochem, Billerica, MA, USA), SD-1029 (Santa Cruz Biotechnology, Santa Cruz, CA, USA) and amantadine (Sigma) were used in the present study.

Transfection of shRNA and siRNAs

To stably establish GL37-shLa and control GL37-shC cells, respectively, we used the plasmids shRNA-La (shLa) and shRNA-control (shC) purchased from Santa Cruz. After electroporation of the plasmids, GL37 cells were placed in 10-mm-well plates (Iwaki Glass, Tokyo, Japan), and treated with 3 μg/mL puromycin for selection of antibiotic-resistant colonies over a 2-week period. We then confirmed the expression of endogenous La by Western blotting. siRNAs against La (siRNA-La), GAPDH (siRNA-GAPDH), PTB (siRNA-PTB), PCBP2 (siRNA-PCBP2), PABP (siRNA-PABP), eIF4E (siRNA-eIF4E), eIF4G (siRNA-eIF4G) and control siRNA (siRNA-control) were purchased from Santa Cruz.

Transfection and luciferase assay

Huh7 cells were seeded in 6-well plates one day before transfecton, and cotransfected with 0.3 μg of the pSV40-HAV-IRES plasmid and 100 nM of each siRNA using Effectene transfection reagent (Qiagen, Hilden, Germany). Forty-eight hours after transfection, cell lysates were collected using a luciferase lysis buffer (Promega, Madison, WI, USA) according to the manufacturer's instructions. Luciferase activity was measured with a luminometer (AB-2200-R; ATTO, Tokyo, Japan).

Western blotting

Cells were lysed in sodium dodecyl sulfate sample buffer, and after sonication, lysates were used for Western blotting analysis. Briefly, proteins were subjected to electrophoresis on 5–20% polyacrylamide gels and transferred onto polyvinylidene difluoride membranes (ATTO, Tokyo, Japan). Membranes were incubated with specific antibodies for La, GAPDH, PTB, PCBP2, PABP, eIF4E, eIF4G and tubulin (Santa Cruz). After washing, membranes were incubated with secondary horse-radish peroxidase–conjugated antibodies. Signals were detected by means of enhanced chemiluminescence (GE Healthcare, Tokyo, Japan) and scanned by image analyzer LAS-4000 and Image Gauge (version 3.1) (Fuji Film, Tokyo, Japan) and Scion Image (Scion) software.

RNA extraction and real-time RT-PCR

After 96 h or 72 h of HAV infection, total RNA was isolated using the RNeasy Mini Kit (Qiagen). One microgram of RNA was reverse-transcribed with the PrimeScript RT reagent (Perfect Real Time; Takara, Otsu, Japan). PCR amplification was performed on cDNA templates using primers specific for HAV (sense primer 5′-AGGCTACGGGTGAAACCTCTTAG-3′ and antisense primer 5′-GCCGCTGTTACCCTATCCAA-3′) [59]. For RNA quantification, real-time PCR was performed using Power SYBR Green Master Mix (Applied Biosystems, Forester City, CA, USA) following the manufacturer's protocol. Data analysis was based on the Standard curve method.

MTS assay

To evaluate cell viability, MTS assays were performed using a Cell Titer Aqueous One Solution Proliferation Assay (Promega) according to the manufacturer's instructions.

Statistical analysis

Statistical analysis was performed using Student's t-test. *P*-values <0.05 were considered statistically significant.

Acknowledgments

We thank Verena Gauss-Müller for providing HAV subgenomic replicon and HuhT7 cells.

Author Contributions

Conceived and designed the experiments: XJ T. Kanda SW OY. Performed the experiments: XJ T. Kanda SW SN KS HS T. Kiyohara KI TW HO. Analyzed the data: XJ T. Kanda SW HS T. Kiyohara KI TW HO OY. Contributed reagents/materials/analysis tools: HS T. Kanda KI OY. Contributed to the writing of the manuscript: XJ T. Kanda T. Kiyohara KI TW HO OY.

References

1. Debing Y, Neyts J, Thibaut HJ (2013) Molecular Biology and Inhibitors of Hepatitis A Virus. Med Res Rev [Epub ahead of print]. doi:10.1002/med.21292. PubMed: 23722879.
2. Kanda T, Yokosuka O, Imazeki F, Fujiwara K, Nagao K, et al. (2005) Amantadine inhibits hepatitis A virus internal ribosomal entry site-mediated translation in human hepatoma cells. Biochem Biophys Res Commun 331: 621–629. doi:10.1016/j.bbrc.2005.03.212. PubMed: 15850805.
3. Jacobsen KH, Wiersma ST (2010) Hepatitis A virus seroprevalence by age and world region, 1990 and 2005. Vaccine 28: 6653–6657. doi:10.1016/j.vaccine.2010.08.037. PubMed: 20723630.
4. Lavanchy D (2013) Viral hepatitis: global goals for vaccination. J Clin Virol 55: 296–302. doi:10.1016/j.jcv.2012.08.022. PubMed: 22999800.
5. Taylor RM, Davern T, Munoz S, Han SH, McGuire B, et al. (2006) Fulminant hepatitis A virus infection in the United States: Incidence, prognosis, and outcomes. Hepatology 44: 1589–1597. doi:10.1002/hep.21439. PubMed: 17133489.
6. Sjogren M (2003) Immunization and the decline of viral hepatitis as a cause of acute liver failure. Hepatology 38: 554–556. doi:10.1053/jhep.2003.50401. PubMed: 12939580.
7. Kanda T, Jeong SH, Imazeki F, Fujiwara K, Yokosuka O (2010) Analysis of 5′ nontranslated region of hepatitis A viral RNA genotype I from South Korea: comparison with disease severities. PLoS One 5: e15139. doi:10.1371/journal.pone.0015139. PubMed: 21203430.
8. Wu S, Nakamoto S, Kanda T, Jiang X, Nakamura M, et al. (2014) Ultra-deep sequencing analysis of the hepatitis A virus 5′-untranslated region among cases of the same outbreak from a single source. Int J Med Sci 11: 60–64. doi:10.7150/ijms.7728. PubMed: 24396287.
9. Baugh JM, Garcia-Rivera JA, Gallay PA (2013) Host-targeting agents in the treatment of hepatitis C: a beginning and an end? Antiviral Res 100:555–561. doi: 10.1016/j.antiviral.2013.09.020. PubMed: 24091203.
10. Malcolm BA, Lowe C, Shechosky S, McKay RT, Yang CC, et al. (1995) Peptide aldehyde inhibitors of hepatitis A virus 3C proteinase. Biochemistry 34: 8172–8179. PubMed: 7794931.
11. Morris TS, Frormann S, Shechosky S, Lowe C, Lall MS, et al. (1997) In vitro and ex vivo inhibition of hepatitis A virus 3C proteinase by a peptidyl monofluoromethyl ketone. Bioorg Med Chem 5: 797–807. doi:10.1016/S0968-0896(97)88649-X. PubMed: 9208091.
12. Huang Y, Malcolm BA, Vederas JC (1999) Synthesis and testing of azaglutamine derivatives as inhibitors of hepatitis A virus (HAV) 3C proteinase. Bioorg Med Chem 7: 607–619. doi:10.1016/S0968-0896(99)00006-1. PubMed: 10353640.
13. Lall MS, Karvellas C, Vederas JC (1999) Beta-lactones as a new class of cysteine proteinase inhibitors: inhibition of hepatitis A virus 3C proteinase by N-Cbz-serine beta-lactone. Org Lett 1999; 1: 803–806. PubMed: 10823207.
14. Lall MS, Ramtohul YK, James MN, Vederas JC (2002) Serine and threonine beta-lactones: a new class of hepatitis A virus 3C cysteine proteinase inhibitors. J Org Chem 67: 1536–1547. doi:10.1021/jo0109016. PubMed: 11871884.
15. Yin J, Cherney MM, Bergmann EM, Zhang J, Huitema C, et al. (2006) An episulfide cation (thiiranium ring) trapped in the active site of HAV 3C proteinase inactivated by peptide-based ketone inhibitors. J Mol Biol 361: 673–686. doi:10.1016/j.jmb.2006.06.047. PubMed: 16860823.
16. Kanda T, Kusov Y, Yokosuka O, Gauss-Müller V (2004) Interference of hepatitis A virus replication by small interfering RNAs. Biochem Biophys Res Commun 318: 341–345. doi:10.1016/j.bbrc.2004.03.194. PubMed: 15120607.
17. Kanda T, Zhang B, Kusov Y, Yokosuka O, Gauss-Müller V (2005) Suppression of hepatitis A virus genome translation and replication by siRNAs targeting the internal ribosomal entry site. Biochem Biophys Res Commun 330: 1217–1223. doi:10.1016/j.bbrc.2005.03.105. PubMed: 15823573.
18. Kusov Y, Kanda T, Palmenberg A, Sgro JY, Gauss-Müller V (2006) Silencing of hepatitis A virus infection by small interfering RNAs. J Virol 80: 5599–5610. doi:10.1128/JVI.01773-05. PubMed: 16699041.
19. Yoshiba M, Inoue K, Sekiyama K (1994) Interferon for hepatitis A. Lancet 343: 288–289. doi:10.1016/S0140-6736(94)91132-0. PubMed: 7507543.
20. Vallbracht A, Hofmann L, Wurster KG, Flehmig B (1984) Persistent infection of human fibroblasts by hepatitis A virus. J Gen Virol 65: 609–615. doi:10.1099/0022-1317-65-3-609. PubMed: 6321640.
21. Yang L, Kiyohara T, Kanda T, Imazeki F, Fujiwara K, et al. (2010) Inhibitory effects on HAV IRES-mediated translation and replication by a combination of amantadine and interferon-alpha. Virol J 7:212. doi:10.1186/1743-422X-7-212. PubMed: 20815893.
22. Kanda T, Wu S, Kiyohara T, Nakamoto S, Jiang X, et al. (2012) Interleukin-29 suppresses hepatitis A and C viral internal ribosomal entry site-mediated translation. Viral Immunol 25: 379–386. doi:10.1089/vim.2012.0021. PubMed: 23035851.
23. Widell A, Hansson BG, Oberg B, Nordenfelt E (1986) Influence of twenty potentially antiviral substances on in vitro multiplication of hepatitis A virus. Antiviral Res 6:103–112. PubMed: 3010855.
24. Crance JM, Biziagos E, Passagot J, van Cuyck-Gandré H, Deloince R (1990) Inhibition of hepatitis A virus replication in vitro by antiviral compounds. J Med Virol 31: 155–160. PubMed: 2167349.
25. Debing Y, Kaplan GG, Neyts J, Jochmans D (2013) Rapid and convenient assays to assess potential inhibitory activity on in vitro hepatitis A replication. Antiviral Res 98: 325–331. doi:10.1016/j.antiviral.2013.03.016. PubMed: 23528258.
26. Ching KZ, Nakano T, Chapman LE, Demby A, Robertson BH (2002) Genetic characterization of wild-type genotype VII hepatitis A virus. J Gen Virol 83: 53–60. PubMed: 11752700.
27. Cordes S, Kusov Y, Heise T, Gauss-Müller V (2008) La autoantigen suppresses IRES-dependent translation of the hepatitis A virus. Biochem Biophys Res Commun 368: 1014–1019. doi:10.1016/j.bbrc.2008.01.163. PubMed: 18282467.
28. Schultz DE, Hardin CC, Lemon SM (1996) Specific interaction of glyceraldehyde 3-phosphate dehydrogenase with the 5′-nontranslated RNA of hepatitis A virus. J Biol Chem 271: 14134–14142. doi:10.1074/jbc.271.24.14134. PubMed: 8662893.
29. Yi M, Schultz DE, Lemon SM (2000) Functional significance of the interaction of hepatitis A virus RNA with glyceraldehyde 3-phosphate dehydrogenase (GAPDH): opposing effects of GAPDH and polypyrimidine tract binding protein on internal ribosome entry site function. J Virol 74: 6459–6468. PubMed: 10864658.
30. Venkatramana M, Ray PS, Chadda A, Das S (2003) A 25 kDa cleavage product of polypyrimidine tract binding protein (PTB) present in mouse tissues prevents PTB binding to the 5′ untranslated region and inhibits translation of hepatitis A virus RNA. Virus Res 98: 141–149. doi:10.1016/j.virusres.2003.09.004. PubMed: 14659561.
31. Kanda T, Gauss-Müller V, Cordes S, Tamura R, Okitsu K, et al. (2010) Hepatitis A virus (HAV) proteinase 3C inhibits HAV IRES-dependent translation and cleaves the polypyrimidine tract-binding protein. J Viral Hepat 17: 618–623. doi:10.1111/j.1365-2893.2009.01221.x. PubMed: 19889140.
32. Graff J, Cha J, Blyn LB, Ehrenfeld E (1998) Interaction of poly(rC) binding protein 2 with the 5′ noncoding region of hepatitis A virus RNA and its effects on translation. J Virol 72: 9668–9675. PubMed: 9811700.
33. Zhang B, Morace G, Gauss-Müller V, Kusov Y (2007) Poly(A) binding protein, C-terminally truncated by the hepatitis A virus proteinase 3C, inhibits viral translation. Nucleic Acids Res 35: 5975–5984. doi:10.1093/nar/gkm645. PubMed: 17726047.
34. Ali IK, McKendrick L, Morley SJ, Jackson RJ (2001) Activity of the hepatitis A virus IRES requires association between the cap-binding translation initiation factor (eIF4E) and eIF4G. J Virol 75: 7854–7863. doi:10.1128/JVI.75.17.7854-7863.2001. PubMed: 11483729.
35. Borman AM, Kean KM (1997) Intact eukaryotic initiation factor 4G is required for hepatitis A virus internal initiation of translation. Virology 237: 129–136. doi:10.1006/viro.1997.8761. PubMed: 9344915.
36. Redondo N, Sanz MA, Steinberger J, Skern T, Kusov Y, et al. (2012) Translation directed by hepatitis A virus IRES in the absence of active eIF4F complex and eIF2. PLoS One 7: e52065. doi:10.1371/journal.pone.0052065. PubMed: 23272212.
37. Wolin SL, Cedervall T (2002) The La protein. Annu Rev Biochem 71: 375–403. PubMed: 12045101.
38. Madore SJ, Wieben ED, Pederson T (1984) Eukaryotic small ribonucleoproteins. Anti-La human autoantibodies react with U1 RNA-protein complexes. J Biol Chem 259: 1929–1933. PubMed: 6229541.